Highlighting a perspective written by Ms. Cuc Mai Thi Kim (University of Oulu-Finland), Dr. Lahoucine Atourki (Mohammed V University-Morocco), Dr. Mouad Ouafi (Mohammed VI Polytechnic University-Morocco) and Dr. Syed Ghufran Hashmi (University of Oulu-Finland).

A synopsis of progressive transition in precursor inks development for metal halide perovskites-based photovoltaic technology

In recent years, a variety of configurations for PSC technology have been reported, where intelligent inks of perovskite precursors have been formulated to facilitate novel designs with impressive solar-to-electrical energy conversions and promising stability. The perspective highlights the evolution of these novel perovskite precursor ink formulations, and discusses the emerging trends in developing efficient, scalable, and robust PSC technology.

As featured in:

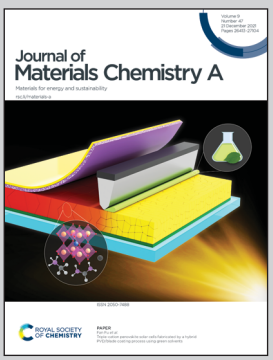

See Syed Ghufran Hashmi *et al.*, *J. Mater. Chem. A*, 2021, **9**, 26650.

ROYAL SOCIETY OF CHEMISTRY

rsc.li/materials-a

Registered charity number: 207890

Journal of Materials Chemistry A

ROYAL SOCIETY OF CHEMISTRY

PERSPECTIVE

View Article Online
View Journal | View Issue

Cite this: J. Mater. Chem. A, 2021, 9, 26650

A synopsis of progressive transition in precursor inks development for metal halide perovskites-based photovoltaic technology

Cuc Mai Thi Kim,[a] Lahoucine Atourki,[b] Mouad Ouafi[cd] and Syed Ghufran Hashmi *[a]

Perovskite solar cell (PSC) technology has received considerable attention due to the rapid escalation of their solar-to-electrical energy conversion, which has recently surpassed 25% for lab-sized solar cells. Other benefits such as their fabrication through solution processing enable new opportunities for scaling up and rapid production. These features may play a key role in realizing quick installations worldwide, helping to meet the global energy production and consumption demand with a realistic energy pay-back time. This report provides an overview of the progress in developing liquid precursor inks for producing a variety of organic–inorganic halide perovskite-based light absorbing layers. In recent years, a variety of configurations for PSC technology have been reported, where intelligent inks of perovskite precursors have been formulated to facilitate novel designs with impressive solar-to-electrical energy conversions and promising stability. This report highlights the evolution of these novel perovskite precursor ink formulations, and discusses the emerging trends in developing efficient, scalable, and robust PSC technology. Moreover, the classification, advantages, and limitations of various types of perovskite precursor ink are addressed. Specifically, single- and multi-cation-based ink formulations are discussed in relation to their impact on producing efficient solar cells, which provides an overview of the recent progress in the development of this emerging and low-cost solar cell technology. Overall, this synopsis provides the current state of the art in designing novel perovskite precursor inks to be used in producing high performance, efficient, scalable, and stable configurations of perovskite solar cell technology.

Received 3rd August 2021
Accepted 15th September 2021

DOI: 10.1039/d1ta06556d

rsc.li/materials-a

[a]Microelectronics Research Unit, Faculty of Information Technology & Electrical Engineering, University of Oulu, P. O. Box 8000, FI-90014, Finland. E-mail: ghufran.hashmi@oulu.fi
[b]MANAPSE Lab, Faculty of Science, Mohammed V University in Rabat, Morocco
[c]CBS, Mohammed VI Polytechnic University, Ben Guerir, Morocco
[d]LMER, Faculty of Science, Ibn Zohr University, Agadir, Morocco

Cuc Thi Mai Kim is currently pursuing her doctoral degree at the Microelectronics Research Unit of the University of Oulu, Finland. She received her M.S. degree in Engineering and Technology from Kumoh National Institute of Technology, South Korea. Before that she completed her Bachelor of Science degree from Vietnam National University, Vietnam. Her research interests include solar cells and water splitting.

Lahoucine Atourki is currently working as an Assistant Professor at the Department of Physics, Mohammed V University in Rabat, Morocco. His research is centered on the growth and characterization of nanomaterials for energy conversion. Houcine's current interest is developing and understanding 2D electronic passivation of 3D perovskites for solar cell applications. Houcine has a Ph.D. degree in Physics from Ibn Zohr University, Morocco. He has also worked as a post-doctoral researcher at the School of Materials Science and Engineering at Georgia Institute of Technology (USA).

1. Introduction

The growing population and resulting human activity continue to increase energy consumption, imposing new challenges for energy supply and production. Solutions must meet sustainable production criteria, especially under the current climate change scenarios.[1,2] These stringent conditions have become a source of intense motivation for researchers worldwide to develop clean and alternative energy production schemes focused on reducing greenhouse gas effects and environmental pollution.[3,4]

Among the various renewable energy sources, photovoltaics has been considered as a potential source for providing clean, silent, and affordable energy with high solar-to-electrical energy conversion.[5–7] Despite the increase in installations of dominant Si-based photovoltaic systems, these have various limitations such as saturated performance for bulk outdoor electricity production, limited aesthetics for modern architecture-based building integrated photovoltaic (BIPV) applications, and non-eco-friendly and high energy consumption-based production methods. Moreover, they display limited performance under low light intensity conditions; efficient conversion of electrical energy under simulated light is needed to energize maintenance-free internet of things (IoT) devices and portable electronics.[8–11]

In this regard, third generation-based photovoltaic (PV) technologies such as dye-sensitized solar cells (DSSCs), organic solar cells (OSCs) and perovskite solar cells (PSCs) offer numerous advantages over Si-based PV systems.[9–11] For example, they provide flexibility in designing solar cells and modules in a variety of sizes, their fundamental materials are abundantly available, and they are fabricated with non-vacuum-based scalable production methods such as established slot-die coating, screen printing or inkjet printing-based material deposition technologies.[12,13] Such unique features make these next generation-based PV technologies a potential source for energizing modern electronics and utilizing their integration in the next generation of BIPV products. They also provide the possibility to produce bulk electricity with much higher solar-to-electrical energy conversion efficiencies compared to stand-alone Si-based PV systems, for example when smartly used in tandem configurations or installed outdoors under natural climatic conditions.[14–16]

Among these next generation-based PV technologies, PSCs have received considerable attention due to the rapid escalation of their solar-to-electrical energy conversion, which has recently surpassed 25%.[17] In addition to these reported improvements in conversion efficiencies, other benefits such as their fabrication through solution processing enable new opportunities for scaling up and rapid production.[18] Importantly, this may play a key role in realizing quick installations worldwide, thus providing a realistic way of meeting the global energy production and consumption demand.[19,20]

This report provides an overview of the progress in developing liquid precursor inks for producing a variety of organic–inorganic halide perovskite-based light absorbing layers in emerging PSC technology. Many configurations for perovskite solar cell technology have been reported in recent years. Specifically, intelligent inks of perovskite precursors have been

Mouad Ouafi received his Doctoral Degree in Physics, with specialization in Materials and Renewable Energies from Mohammed V University of Rabat, Morocco. He worked on perovskite materials to be used as absorber layers for solar cell applications. He then moved to Mohammed VI Polytechnic University, Morocco to work as a Post-doctoral researcher. His current research interests include luminescent solar concentrators and perovskite solar cells.

Syed Ghufran Hashmi is Tenure Track Assistant Professor in Printed Electronics at the Microelectronics Research Unit of the University of Oulu, Finland. He has received numerous prestigious fundings in the capacity of Project Leader and Principal Investigator from top funding organizations including the Technology Industries of Finland Centennial Foundation, Jane and Aatos Erkko Foundation, Business Finland and Academy of Finland for the research and development of the next generation of photovoltaic devices such as dye-sensitized solar cells and perovskite solar cells. He received his D.Sc. degree in Engineering Physics from Aalto University – Finland in 2014. Before that, he received his M.Sc. degree in Micro- and Nanotechnology from Helsinki University of Technology – Finland in 2009 and BS Degree in Biomedical Engineering from Sir Syed University of Engineering and Technology – Pakistan in 2002. He has authored nearly 30 scientific publications, which have received >970 citations. His research interests include solar cells, printed electronics, energy harvesting, solar fuels, printable batteries and supercapacitors.

formulated to facilitate novel designs with impressive solar-to-electrical energy conversions and promising stability.[21–24] This report highlights the evolution of these novel perovskite precursor ink formulations and discusses the emerging trends towards developing efficient and robust PSC technology. In addition, the classification, advantages, and limitations of various types of perovskite precursor ink are addressed. Single- and multi-cation-based ink formulations are discussed in light of their impact on producing efficient solar cells. Progress in developing lead (Pb)-free precursor inks is also reviewed, as well as the scalable precursors that have been identified for producing large-area solar modules in a variety of configurations with popular scalable fabrication methods. Overall, this review provides the most up-to-date advancements being made in designing novel perovskite precursor inks for producing high performance, efficient, scalable, and stable configurations of perovskite solar cell technology.

2. Role of precursor inks in establishing the current state of the art for conversion efficiencies of PSC technology

The progressive advances in PSC solar-to-electrical conversion efficiencies (Fig. 1) may be attributed to many factors, for example, the known knowledge of design principles for producing solid state DSSCs (ssDSSCs),[25,26] optimizing the active layer thicknesses for improving the diffusion lengths of carriers,[27–29] or even proposing intelligent strategies for minimizing both the radiative and non-radiative losses observed in device architectures.[30–35]

The advances in designing novel perovskite precursor inks[36–39] have played a key role in addressing the aforementioned key issues, thus leading to extraordinary improvements in solar-to-electrical energy conversions in recent years (Fig. 1).

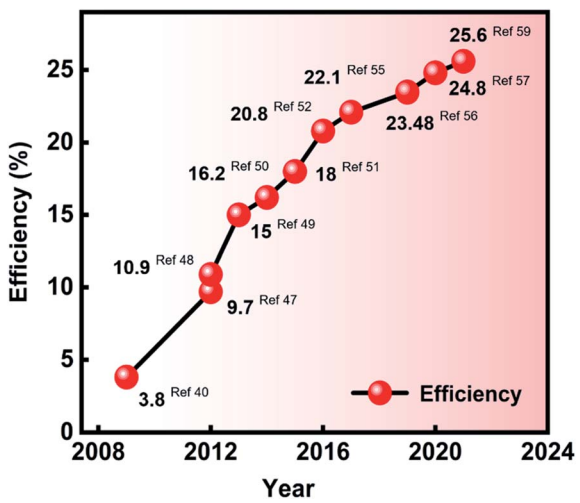

Fig. 1 Solar-to-electrical conversion efficiency evolution of lab-sized perovskite solar cells.

The striking discovery of potential applications of perovskite-based light harvesters in photovoltaics was preliminarily reported by formulating two types of precursor ink.[40] Briefly, CH_3NH_3Br and $PbBr_2$ were dissolved in *N*,*N*-dimethylformamide (DMF) solvent, while CH_3NH_3I and PbI_2 were mixed in γ-butyrolactone (GBL) as a high viscosity solvent, cast on a TiO_2 nanocrystalline film *via* the spin coating method (also known as the single-step deposition method).[41–43] The solar cells produced in a liquid junction DSSC assembly fashion resulted in 3.81% solar-to-electrical energy conversion when tested under full sunlight illumination.[40]

Following these findings, several additional reports have assessed other novel precursor inks including lead-based compounds. For example, lead iodide (PbI_2) or lead chloride ($PbCl_2$) have been combined with other organic–inorganic salts such as methylammonium iodide (CH_3NH_3I) or cesium iodide (CsI) and a variety of solvents to further improve the solar-to-electrical conversion efficiencies of the fabricated solar cells.[44–46]

Among these investigations, the study by Kim *et al.* mimics the solid-state dye-sensitized solar cell (ssDSSC) device design, in which the TiO_2-based electron transport layer (ETL) was first infiltrated with MAI and PbI_2 containing a perovskite precursor ink with a GBL solvent kept overnight while stirring at 60 °C.[47] The solid-state cell architecture was further processed *via* casting a hole transporting layer (HTL), *i.e.* Spiro-OMeTAD, followed by thermal evaporation of gold to produce the final contact layer. Interestingly, the fabricated solar cells not only exhibited far higher conversion efficiencies (>9%) compared to previous reports, but they also exhibited striking photovoltaic performance stability during periodic measurements when tested without encapsulation for a period of 500 hours in air combined with room temperature (RT)-based ecological conditions.

Building on the outcomes of the aforementioned research, >10% conversion efficiencies were promptly demonstrated for lab-sized PSC devices, also by incorporating a mixed cation-based perovskite precursor solution ink that was used to achieve the perovskite light absorbing layer through a single-step spin coating method.[48]

Unlike the single-step processing-based precursor inks, the pioneering work reported by Burschka *et al.* used a two-step processing scheme. In this approach, the perovskite-based light absorbing layer in the PSC device structure was achieved by fabricating two individual solutions.[49] The first precursor ink was obtained by dissolving PbI_2 in DMF and was kept at 70 °C before the infiltration in step 1 through spin coating. Next, glass electrodes containing the PbI_2-infiltrated electron transport layer (ETL, TiO_2) were dipped into a solution of MAI containing 2-propanol solvent for 20 seconds to obtain the desired perovskite crystal-based light harvesting layer. Striking solar-to-electrical conversion efficiencies reached 15% due to achieving a controlled perovskite crystal morphology in response to the previously reported single-step mixed halide perovskite inks.[49]

Since the description of these initial techniques, progressive enhancements in conversion efficiencies have continued. The solar-to-electrical energy conversion milestone of 25% was

Table 1 List of the numerous halide perovskite precursor inks used in the gradual enhancements in the solar-to-electrical conversion efficiencies of lab-sized PSCs in recent years

Perovskite precursor ink recipe	Method of deposition	Cell structure	Active area (cm^2)	η (%)	Ref.
$MAPbI_3$-8 wt% of MAI and PbI_2 in GBL $MAPbBr_3$-20 wt% of MABr and $PbBr_2$ in DMF	Spin-coating	DSSC liquid cell fashion Glass/FTO/TiO_2/PVK/thermoplastic separator film/Pt-coated FTO-glass	0.238	3.81	40
0.395 g synthesized MAI and 1.157 g PbI_2 mixed in GBL (2 mL) at 60 °C overnight with stirring	Spin-coating	All-solid-state PSC: glass/FTO/c-TiO_2/m-TiO_2/PVK/Spiro-OMeTAD/Au	0.207	9.7	47
MAI and $PbCl_2$ (3 : 1 molar ratio) dissolved in anhydrous DMF → $MAPbI_2Cl$ (20 wt%)	Spin-coating	Glass/FTO/c-TiO_2/m-Al_2O_3/PVK/Spiro-OMeTAD/Au	0.09	10.9	48
PbI_2 in DMF (462 mg mL^{-1}) (stirring at 70 °C) (spin coating) MAI in IPA (10 mg mL^{-1}) (dipping)	Two-step deposition[a]	Glass/FTO/c-TiO_2/m-TiO_2/PVK/Spiro-OMeTAD/Au	0.285	15	49
0.8 M $MAPb(I_{1-x}Br_x)_3$ (x = 0.1–0.15) stirred in a mixture of GBL and DMSO (7 : 3, v/v) at 60 °C for 12 h	Spin-coating	Glass/FTO/c-TiO_2/m-TiO_2-PVK nanocomposite layer/PVK upper layer/PTAA/Au	0.094	16.2	50
H_2O (0.5–4 wt% *vs.* DMF) added to PbI_2/DMF (0.8 M) MAI in IPA (50 mg mL^{-1})	Two-step deposition[b]	Glass/ITO/PEDOT:PSS/PVK/$PC_{71}BM$/Ca/Al	0.1	18	51
FAI, PbI_2, MABr, and $PbBr_2$ in mixed solvent DMF and DMSO (4 : 1, v/v) $R_{PbI_2/FAI}$ (molar ratio) varies from 0.85 to 1.54 $R_{PbI_2/PbBr_2}$ fixed at 5.67 $R_{MABr/PbBr_2}$ fixed at 1 : 1 Best: $R_{PbI_2=FAI}$ = 1 : 05, corresponding to a 3% weight excess of PbI_2 in the perovskite	Spin-coating	Glass/FTO/c-TiO_2/m-TiO_2/PVK/Spiro-OMeTAD/Au	0.16	20.8	52
$(FAI)_{0.81}(PbI_2)_{0.85}(MAPbBr_3)_{0.15}$ precursor solution prepared in a glovebox from 1.35 M Pb^{2+} (PbI_2 and $PbBr_2$) in a mixed solvent of DMF, NMP and DMSO (where the molar ratio of DMF/DMSO is 5 : 1, and the molar ratio of Pb^{2+}/$[(DMSO)_{0.8}(NMP)_{0.2}]$ is 1 : 1)	Spin-coating	Glass/FTO/c-TiO_2/m-TiO_2/PVK/Spiro-OMeTAD/Au	0.1051	21.6	53
RbI, pre-dissolved as a 1.5 M stock solution in DMF : DMSO 4 : 1 (v/v), added to the Cs/FA/MA triple cation perovskite to achieve the desired quadruple composition	Spin-coating	Glass/FTO/c-TiO_2/m-TiO_2/PVK/Spiro-OMeTAD/Au	0.16	21.6 (stabilized)	54
PbI_2 (1.30 M) containing 2.5 mol% $PbBr_2$ dissolved in a 1 mL mixture of DMF and DMSO (8 : 2, v/v) at 80 °C → Spin coating to form a $PbI_2(PbBr_2)$–DMSO film In the second step, a solution of FAI (80 mg) and MABr (10 mg), containing iodide ions (I^-) (0–5 mM) dissolved in 1 mL IPA was spin coated	Two-step deposition[b]	Glass/FTO/c-TiO_2/m-TiO_2-PVK nanocomposite layer/PVK upper layer/PTAA/Au	0.096	22.1	55
Mixing 1.139 mg mL^{-1} $FAPbI_3$ (0.8 M solution of PbI_2 and FAI in GBL) in a mixture of DMF and DMSO in a 4 : 1 ratio, v/v. MACl added in the range of 0–50 mol%	Spin-coating	Glass/FTO/c-TiO_2/m-TiO_2/PVK/Spiro-OMeTAD/Au	0.0804	23.48	56
1.550 mg mL^{-1} $FAPbI_3$ and 61 mg MACl dissolved in a mixture of DMF and DMSO (4 : 1, v/v)	Spin-coating	Glass/FTO/c-TiO_2/m-TiO_2/PVK/HTM/Au HTMs: two fluorinated isomeric analogs of Spiro-OMeTAD (Spiro-mF and Spiro-oF)	0.0819	24.8 and 22.31 (a large area of 1 cm^2 on the active area)	57
Perovskite solution was prepared by mixing 1.53 M PbI_2, 1.4 M FAI, 0.5 M MACl (as an additive), and 0.0122 M − 0.153 M $MAPbBr_3$ in DMF : DMSO = 8 : 1 Bulk perovskite layer is passivated with a 2D perovskite	Spin-coating	Glass/FTO/SnO_2/PVK/Spiro-OMeTAD/Au	0.0937	25.2	58

Table 1 (*Contd.*)

Perovskite precursor ink recipe	Method of deposition	Cell structure	Active area (cm^2)	η (%)	Ref.
For the 2D perovskite passivation, 10 mM of alkylammonium bromide was deposited at 3000 rpm for 30 s The reference perovskite precursor solution was prepared by mixing 1.139 mg $FAPbI_3$ and 35 mol% MACl in a mixture of DMF and DMSO (4 : 1). For the formate-doped $FAPbI_3$ perovskite film, extra FAHCOO was added to the reference solution in the range of 1–4 mol%	Spin-coating	Glass/FTO/c-TiO_2/m-TiO_2/PVK/octylammonium iodide/Spiro-OmeTAD/Au	0.0804	25.6	59

[a] Two-step deposition: step 1 = spin coating, step 2 = dipping. [b] Two-step deposition: step 1 = spin coating, step 2 = spin coating. PVK = perovskite.

recently surpassed for lab-sized PSCs[17] due to the tremendous efforts being made in developing individual components of this solution-processed PV technology. Designing and developing novel precursor inks for producing high quality perovskite-based light absorbing active layers has remained the focus of reaching high performance and striking stability under several simulated and natural climatic conditions. Fig. 1 summarizes the solar-to-electrical energy conversion evolution. Table 1 provides a list of various perovskite precursor inks used to contribute towards enhancing the conversion efficiencies of lab-sized PSCs in recent years.

3. Emerging research trends in perovskite precursor ink development

There are a variety of precursor inks that have been developed by incorporating various novel materials to produce perovskite-based light absorbing active layers. These precursor inks (Fig. 2) can be categorized as classical single-cation based,[60–62] multi-cation based,[63–65] additive based,[53,66–68] or lead-free.[69–71]

Traditional PSC devices have been initially reported with a classical ABX_3-based crystalline perovskite active layer. Here, A generally represents methyl-ammonium $CH_3NH_3^+$, formamidinium $NH_2CH = NH_2^+$ or cesium (Cs)-based monovalent organic or inorganic cations.[40,46] B typically represents Pb^{2+}, Sn^{2+} or even Ge^{2+}-based divalent metal cations, and X_3 shares I^-, Cl^-, Br^- or Fl^- as monovalent anions during the crystal formation of the traditional perovskite-based light absorbing layer.[72,73]

Due to the inherited characteristics such as stable crystal formations,[74–78] good chemical compatibility with other active layers, high efficiency and robust stability under initially simulated environmental conditions,[79,80] single cation-based perovskite precursor inks have been the focus of developing the first generation of lab-sized PSC devices.[81–83] Interestingly, these first-generation precursor inks exhibited strong processing compatibility when incorporated utilizing both the single-step and two-step fabrication schemes to produce lab-sized PSC devices.[84–88] Nevertheless, single-step processable precursor inks have remained the preferred choice for scaling up various device designs of PSC technology.[89,90]

Recently, trends of multi-cation-based ink formulations have also emerged, not only for suppressing non-radiative losses but also for achieving high performance and better stability. This has mainly been achieved through large grain boundary-based crystal formulations, along with physical and chemical stabilities of perovskites as light harvesters in PSCs.[63,91–94]

Bi *et al.* demonstrated a unique multi-cation-based halide precursor ink by incorporating multi-cations such as formamidinium iodide (FAI) and methylammonium bromide (MABr) salts with lead bromide ($PbBr_2$) and PbI_2. These were dissolved in a mixed solvent system containing dimethyl formamide (DMF) and dimethyl sulfoxide (DMSO) solvents. This recipe of perovskite precursor ink resulted in PSC devices with >20% conversion efficiency.[52]

In addition to multi-cations, other novel additives have also been introduced in precursor inks to overcome/achieve some of the key bottlenecks and milestones related to technological

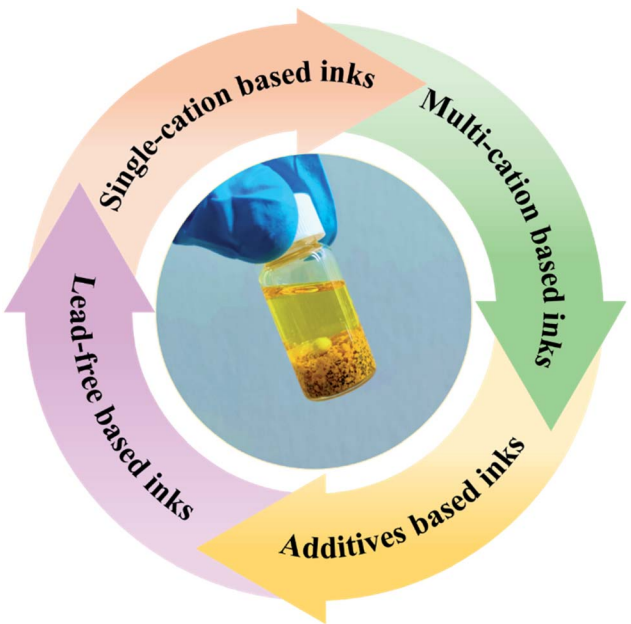

Fig. 2 General classification trends of perovskite precursor inks that have emerged in recent years.

challenges and long-term performance stabilities necessary for the successful commercialization of PSC technology.[95–99] In this regard, one ground-breaking research study in terms of designing a novel perovskite precursor ink was reported by Mei and co-workers. The striking mesoscopic carbon-based printable perovskite solar cell (CPSC) device design featured the introduction of an additive, *i.e.* 5-ammonium valeric acid iodide (5-AVAI), in the solution recipe of the traditional perovskite precursor ink.[21] The additive (5-AVAI) induces control over the crystallization process during the infiltration of the formulated perovskite ink in a much thicker and more porous structure compared to the traditional PSC device configurations.[100–102] As a result, the formulated ink contributed to surpassing the first >1000 hours stability test of these carbon-based printable perovskite solar cells when exposed to ambient air under full sunlight intensity conditions.[21] The promising characteristics of this device design have yielded beneficial features, including successful scaling up and promising conversion efficiencies demonstrated in PSCs ranging from lab-sized to various module sizes, along with robust stability when deployed under various natural and simulated climatic conditions.[103–105] Interestingly, 5-AVAI containing a novel precursor ink formulation has also been incorporated with scalable material deposition methods such as inkjet printing or slot-die coating-based technologies.[106–108]

In contrast to CPSCs, Bi and co-workers used polymer poly(methyl methacrylate) (PMMA) as the templating agent-based additive in the multi-cation-based precursor ink. They demonstrated perovskite films of high electronic quality for producing very high conversion efficiency (>21%) in one of the traditional mesoporous n–i–p PSC devices.[53] With the impressive solar-to-electrical energy conversion, the photovoltaic parameters were shown to have an influence upon adjusting the concentration of PMMA, where the champion efficiencies (21.6%) were recorded with a controlled nucleation and crystal growth based light absorbing layer when a specific concentration (0.6 mg mL^{-1}) was used in the fabricated perovskite precursor ink.[53]

Moreover, the concept of introducing ionic liquids (ILs) in perovskite precursor inks as one of the other promising additive components has also received attention for achieving high performance and robust stability when tested in several configurations.[99,109–113] For example, Bai and co-workers introduced 1-butyl-3-methylimidazolium tetrafluoroborate ($BMIMBF_4$) ionic liquid in the multi-cation perovskite precursor ink. They observed striking efficiencies of 20% at the steady state when fabricated as p–i–n configuration-based PSC devices containing this IL-based perovskite light absorbing layer.[109] The inclusion of $BMIMBF_4$ IL as an additive shows promise for influencing the crystallinity and reducing the defects in the incorporated perovskite-based light absorbing layer in the fabricated PSCs. This also contributed to the stability results when exposed to full-spectrum sunlight in air (RH 40–50%) at 60–65 °C, or full-spectrum sunlight at 70–75 °C based on the environmental testing conditions.[109]

Importantly, incorporating ILs in perovskite precursor inks not only offers control over crystallization dynamics and improved charge transport in the perovskite light absorbing layers, but it also provides a possibility for using them as green solvents for realizing the steps towards making PSCs an eco-friendly technology.[114–117] For example, Chao and co-workers demonstrated a novel precursor ink utilizing an eco-friendly IL, *i.e.* methylammonium acetate (MAAc), as one of the possible green solvents for producing an efficient and pinhole-free perovskite light absorbing layer. This method revealed promising environmental stability for a period of more than 3000 hours under high humidity (60–80%) conditions.[115] Motivated by such promising findings, both n–i–p and p–i–n configuration-based PSCs were fabricated by incorporating this novel precursor ink that showed promising solar-to-electrical energy conversions (~16–20%). Notably, 20.05% is the champion conversion efficiency marked for the n–i–p based planar PSC device design under full sunlight illumination. More impressively, the non-sealed fabricated PSCs also exhibited striking long-term photovoltaic performance stability by retaining 93% of the initial device efficiency under air for more than 1000 hours. A minor deviation (<20%) in the initially achieved efficiency was observed after 700 hours of testing under light stress under the conditions maintained in the glovebox.[115]

Despite the numerous striking features acknowledged for this emerging low-cost PV technology, one of the key concerns raised relates to incorporating hazardous and toxic compounds such as lead (Pb)-based compounds, which have thus far remained an essential element in producing high performance PSCs.[118–120] Use of Pb in a PSC, however, restricts its deployments in many portable and consumer electronics-based applications since it may leak from such devices and cause bodily harm.[121] Similarly, deploying PSCs outdoors for bulk electricity generation also requires robust encapsulation procedures due to the solubility of Pb as a heavy metal in water. This may generate a negative environmental impact as indicated in several life cycle assessment reports for PSC technology.[122–124] Hence, efforts are being made to either reduce or completely replace Pb-based compounds from the next generation of PSC devices.[125,126]

In this regard, the emerging trends for demonstrating lead-free precursor formulations include tin (Sn)-[127–129] or germanium (Ge)-based halide perovskite precursor inks.[130,131] Similarly, trivalent antimony (Sb^{3+})-[132–134] or bismuth (Bi)-[135–137] based perovskite precursor formulations have also been explored as possible alternatives for replacing hazardous and toxic lead-based halide perovskite precursor inks.[125,126,138]

Among these formulations, Sn-based formulations have thus far contributed to a gradual increase in the solar-to-electrical conversion efficiencies,[128,129,139–141] which has recently exceeded above 13% when tested in inverted p–i–n device design-based PSCs under full sun illumination.[127] Nevertheless, the long-term photovoltaic performance stability was not demonstrated, hence further investigations are needed for producing robust lead-free PSCs in the near future. Table 2 summarizes versatile ink formulations that have been incorporated in many device designs in recent years to produce high performance perovskite solar cell devices.

Table 2 Classifications of perovskite precursor inks highlighting the champion photovoltaic performance with some of the best recipes used in various PSC configurations

	Perovskite precursor inks	Deposition method	Perovskite	η (%)	Stability	Ref.
Single cation	1.6 M $MAPbI_3$ (MAI : PbI_2 molar ratio 1 : 1) in GBL, stirred overnight at 60 °C	Solution space-limited inverse-temperature crystal growth method	$MAPbI_3$ single crystal	21.09	—	142
	663 mg of the synthesized $FAPbI_3$ powder and 71 μL of DMSO (molar ratio 1 : 1) in 568 μL of DMF	Spin coating	$FAPbI_3$	21.07 (certified)	80% of the original is retained after 30 days (in the dark, RH 20%) and 92% of the original is retained after 100 min (1 sun, RH 30%, without encapsulation)	143
	The 0.6 M $CsPbI_3$ perovskite precursor was prepared by dissolving stoichiometric CsI, PbI_2, and xDMAI in a 1 : 1 : x molar ratio in DMF (x = 0.5, 0.7, 1.0 and 1.5)	Spin coating	Phenyltrimethylammonium chloride (PTACl) passivated $CsPbI_3$	19.03	90% of the original is retained after 500 h continuous white light LED illumination (100 mW cm^{-2}) in a N_2 glove without encapsulation	144
Multi cations	Mixing FAI (1 M), PbI_2 (1.1 M), MABr (0.2 M) and $PbBr_2$ (0.2 M) in anhydrous DMF : DMSO 4 : 1 (v/v). Then CsI, pre-dissolved as a 1.5 M stock solution in DMSO, was added to the mixed perovskite precursor to achieve the desired triple cation composition	Spin coating	$Cs_{0.05}(MA_{0.17}FA_{0.83})_{0.95}$-$Pb(I_{0.83}Br_{0.17})_3$	21.1	The device efficiency drops from 20% to 18% where it stays relatively stable for at least 250 h (in a N_2 atmosphere and room temperature under continuous illumination at MPP)	145
	889 mg mL^{-1} of $FAPbI_3$, 33 mg mL^{-1} of $MAPbBr_3$ and 33 mg mL^{-1} of MACl in DMF/DMSO (8 : 1, v/v) mixed solvent	Spin coating	$(FAPb_3)_{0.95}(MAPbBr_3)_{0.05}$	22.7 (certified)	95% of the initial efficiency retained after 1370 h under 1-sun illumination at room temperature (with encapsulation)	146
	1.53 M PbI_2, 1.4 M FAI, 0.11 M $MAPbBr_3$, 0.5 M MACl in DMF : DMSO = 8 : 1 volume ratio	Spin coating	$(FAPbI_3)_{0.92}(MAPbBr_3)_{0.08}$	23.4	The device maintained 85% of its efficiency after 500 h under full solar illumination (AM 1.5G, 100 mW cm^{-2}) without a UV-filter at MPP tracking (with encapsulation) in ambient air	147
	0.02 M GAI, 0.09 M CsI, 0.2 M MABr, 1.1 M FAI, 1.2 M PbI_2, and 0.3 M $PbBr_2$ in anhydrous DMF : DMSO (4 : 1, v/v) mixed solvent	Spin coating	$GA_{0.015}Cs_{0.046}MA_{0.152}$-$FA_{0.787}Pb(I_{0.815}Br_{0.185})_3$	20.96	—	148

Table 2 (*Contd.*)

	Perovskite precursor inks	Deposition method	Perovskite	η (%)	Stability	Ref.
Additives	1.35 M Pb^{2+}(PbI_2 and $PbBr_2$) and 0.6 mg mL^{-1} BrPh-ThR in the mixed solvent of DMF and DMSO (volume ratio 4 : 1)	Spin coating	$(FAI)_{0.81}(PbI_2)_{0.85}(MABr)_{0.15}(PbBr_2)_{0.15}$; (Lewis base BrPh-ThR and Lewis acid bis-PCBM (*N*-(4-bromophenyl)thiourea))	21.7	The unsealed devices remained at 93% of the initial efficiency value in ambient air (10–20% relative humidity) after 3600 h at 20–25 °C, and dropped by 10% after 1500 h under continuous operation at 1-sun illumination and 55 °C in nitrogen with MPPT	149
	Two-step solution process: Mixing 1.3 M PbI_2 in DMF/DMSO (9 : 1, v/v) with 5% CsI Note: for the NaX-containing perovskite film, NaX was added Mixing 0.12 M MAI, 0.05 M MABr, 0.07 M MACl, and 0.23 M FAI in IPA	Spin coating	$(Cs_{0.05}FA_{0.54}MA_{0.41})$-$Pb(I_{0.98}Br_{0.02})_3$; (NaF)	21.46 (21.43% certified)	The unencapsulated device retained over 90% of its initial PCE after 1000 h under MPP tracking and continuous light irradiation with a white LED lamp, 100 mW cm^{-2} in a nitrogen atmosphere	150
	1.139 mg mL^{-1} $FAPbI_3$ in a mixture of DMF and DMSO (4 : 1, v/v). MACl was added in the range 0–50 mol%	Spin coating	MACl additive (40 mol%) was applied in $FAPbI_3$	24.02 (certified 23.48%)	The stability at RT showed 90% retention of the device's initial performance over 1200 h. The 40 °C thermal stability test showed 90% retention of the device's initial performances over 300 h	56
	573.0 mg PbI_2, 197.5 mg MAI, and 13.70 mg 5-AVAI in 1.0 mL GBL	Slot-die coating	5-AVAI in $MAPbI_3$	12.87	—	106
Lead free	Mixing the GeI_2 doped $FA_{0.98}EDA_{0.01}SnI_3$ and GeI_2 doped $EA_{0.98}EDA_{0.01}SnI_3$ precursor solution at a molar ratio of $x = 0$, 0.05, 0.1, 0.2	Spin coating	GeI_2 doped $(FA_{0.9}EA_{0.1})_{0.98}EDA_{0.01}SnI_3$.	13.24	—	127
	First dissolving 129 mg FAI, 39.7 mg MAI, 372.5 mg SnI_2, and 15.7 mg SnF_2 in 875 μL DMF : 125 μL DMSO. Meanwhile, 55.8 mg GeI_2 was dissolved in 200 μL DMF. Different concentrations of GeI_2 (5 mol% and 10 mol%) were subsequently added into the bulk precursor	Spin coating	5 mol% germanium doped $FA_{0.75}MA_{0.25}Sn_{1-x}Ge_xI_3$	7.9	90% of the unencapsulated device's initial efficiency retained over 600 min under constant illumination under ambient conditions	151
	Dissolving AgI, BiI_3, and $[Bi(S_2CAr)_3]$ at the desired ratios in a mixed solvent system (DMSO : DMF : HI, 3 : 1, v/v), to which HI (0.12 vol.) was slowly added dropwise	Spin coating	$Ag_3BiI_{5.92}S_{0.04}$	5.44	When stored in air at room temperature (≈22–24 °C) at RH of 40% under diffuse light, the device showed a promising stability and retained more than 90% of the initial PCE after 45 days	152

4. Research and development trends for advanced scalable precursor inks

Motivated by the successes achieved from solution processed lab-sized PSCs with traditional perovskite precursor inks, efforts have also been made towards scaling up PSC technology on a variety of substrates by designing novel precursor inks with key characteristics as shown in Fig. 3.[153–158] In this regard, spin coating has remained the foremost choice for perovskite precursor ink deposition, as well as for the initial scaling up demonstrations of PSC technology (Table 3).[159–161]

Among these initial pioneering efforts, Matteocci *et al.* demonstrated the first n–i–p structure-based solid-state monolithic module[162] with organometal halide perovskite $CH_3NH_3PbI_{3-x}Cl_x$ ink, produced by dissolving methylammonium iodide CH_3NH_3I and lead chloride $PbCl_2$ in a *N*,*N*-dimethylformamide (DMF)-based solvent. The ink was spin-coated at 2000 rpm for 40 s over the nanocrystalline TiO_2-based electron transport layer (ETL) in air and successively heated at 120 °C for 45 minutes to obtain the final crystalline structure. The fabricated modules exhibited similar (~5.1%) conversion efficiencies when tested with two types of hole transporting layer (Spiro-OMeTAD and poly(3-hexylthiophene-2,5-diyl) (P_3HT) polymer) and thermally evaporated gold (Au)-based contact layers over an active area of 16.8 cm^2.

As a further advancement, Seo *et al.* reported an inverted (p–i–n) structure-based module design with a perovskite ink composed of CH_3NH_3I and PbI_2, which were stirred in a mixture of dimethyl sulfoxide (DMSO) and γ-butyrolactone (GBL)-based solvents at 60 °C for 12 h.[163] The ink was deposited onto a PEDOT:PSS/ITO substrate by a consecutive two-step spin-coating process at 1000 and 4000 rpm for 20 and 60 s, respectively. The toluene in the final spin-stage was dripped onto the substrate during spin coating. The perovskite precursor-coated substrate was then dried on a hot plate at 100 °C. The fabricated module with the phenyl-C61-butyric acid methyl ester (PCBM)-based ETL and Al coated contact layer showed an impressive conversion efficiency (8.7%) over a far larger active area (60 cm^2) when tested under full sunlight illumination.

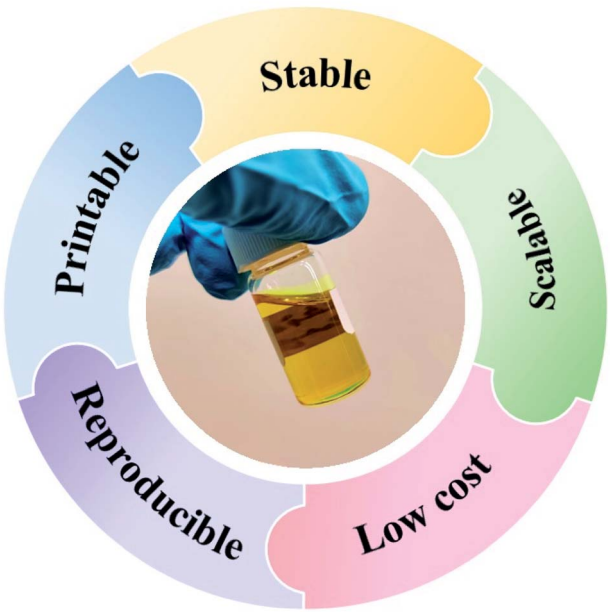

Fig. 3 General characteristics of an efficient perovskite precursor ink.

In addition to these earlier reports of precursor ink development with the spin coating-based material deposition method, advanced single- and two-step processable precursor inks have also been developed and tested with more established scalable approaches (as depicted in Fig. 4), such as blade coating and slot-die coating to fabricate large area perovskite-based solar modules.[164–167] For example, Razza *et al.* used a two-step approach where the pre-heated PbI_2 precursor ink was first coated on ETL layers using a blade coating method followed by rapid evaporation of its solvent (DMF) through an airflow.[164] Next, the perovskite crystalline layer was achieved by directly dipping the substrates containing PbI_2-coated ETL layers into the MAI solution with different dipping times. The perovskite modules fabricated with this approach exhibited 4.3% conversion efficiency under full sunlight illumination over an active area of 100 cm^2.

Deng *et al.* introduced the novel concept of adding a surfactant to the perovskite precursor ink and demonstrated impressive control over the crystallization morphology of the large-area perovskite-based light absorbing layer when deposited with a blade coating scheme.[168] The fabricated modules showed very high (~15%) conversion efficiency when tested under full sunlight illumination with a p–i–n device design. Similarly, Giacomo *et al.* demonstrated slot-die coating of a precursor solution for a perovskite layer, which was prepared under room temperature conditions in an inert N_2 environment.[169] The solution was prepared by dissolving 1 mM of lead compounds and 3 mM of CH_3NH_3I in 1 mL of DMF solvent. The solution was stirred for at least 10 minutes before final use. Slot-die coating of this perovskite precursor ink was performed inside a glovebox, which allowed deposition of a wide range of thicknesses. The wet layer thickness of the perovskite was in the range of 3–4 μm to get a dry layer thickness of 350 nm. With these optimizations, a 12.5 × 13.5 cm^2 module with power conversion efficiencies above 10% over an active area of approximately 152 cm^2 was achieved in the planar n–i–p configuration.[169]

Recently, slot-die coating of a novel perovskite precursor ink containing MAI, PbI_2 and 5-ammonium valeric acid (5-AVAI) in GBL (tested with the drop-casting[170] and inkjet printing methods[107,108]) has also been demonstrated.[106] The fabricated triple mesoscopic printable perovskite solar modules showed an impressive conversion efficiency of 12.87%, which was attained over an active area of 60.08 cm^2 under full sunlight illumination.[106]

Similar scalable demonstrations of organic–inorganic lead halide perovskite-based novel inks with the techniques discussed above have also been utilized to scale up PSC technology on flexible substrates. Flexible modules in various device designs have been developed and reported both by research labs and commercial players in recent years.[171–174] Therefore, there is promising evidence of successful fabrication of the novel organic–inorganic lead halide-based precursor ink formulations for achieving module production, where several device

Table 3 Summary of the scalable device configurations developed in recent years with novel perovskite precursor inks[a]

Ink recipe (PVK)	Method	Device structure	Active area (cm^2)	Module area (cm^2)	η (%)	Ref.
MAI and $PbCl_2$ (molar ratio 3 : 1) in DMF	Spin coating	Glass/FTO/TiO_2/PVK/HTM/Au	16.8	5 × 5	5.1[b]	162
MAI : PbI_2 (molar ratio 1 : 1) in GBL : DMSO (3 : 7, v/v)	Spin coating	Glass/ITO/PEDOT:PSS/PVK/PCBM/LiF/Al	60	10 × 10	8.7[c]	163
PbI_2 in DMF (285 mg mL^{-1}) MAI solution in IPA (10 mg mL^{-1})	Spin coating and dipping	Glass/FTO/c-TiO_2/graphane + m-TiO_2/Go-Li/PVK/Spiro/Au	50.6	10 × 10	12.6[b]	175
PbI_2 : MAI (1 : 1 molar ratio) in GBL 5-AVA-I added to the perovskite solutions in a molar ratio of 1 : 20 (AVA-I to MAI)	Drop casting	Glass/FTO/TiO_2/ZrO_2/carbon/PVK	70	10 × 10	10.75[b]	176
1.2 M MAI and 1.2 M PbI_2 dissolved in GBL For 2D perovskite: 1.2 M AVAI and 1.2 M PbI_2 dissolved in GBL	Drop casting	Glass/FTO/TiO_2/ZrO_2/carbon/PVK	47.6	10 × 10	11.16[b]	177
Mixing 0.07 g 5-AVAI, 4.61 g PbI_2 and 1.59 g MAI in 10.5 mL GBL	Drop casting	Glass/FTO/TiO_2/ZrO_2/carbon/PVK	49	10 × 10	10.4[b]	170
PbI_2 and MAI (1 : 1 molar ratio) in GBL prepared by adding 5-AVAI to obtain a 3% molar ratio between 5-AVAI and MAI	Drop casting	Glass/FTO/TiO_2/ZrO_2/carbon/PVK	198	435.6 (aperture)	6.3[b] (stabilized) (after 2 months since fabrication)	178
Blade coating of PbI_2 in DMF (330 mg mL^{-1}) Dipping into MAI solution (in IPA) (10 mg mL^{-1})	Blade coating	Glass/FTO/c-TiO_2/mp-TiO_2/PVK/P_3HT/Au	100	16 × 11	4.3[b]	164
30 wt% and 45 wt% equimolar ratio of MAI and PbI_2 precursors with different amounts of MACl additive in a mixed solvent (NMP/DMF 9 : 8, v/v)	Blade coating	Glass/FTO/c-TiO_2/PVK/Spiro-OMeTAD/Au	11.09	12.6	13.3[b] (stabilized)	179
0.8 M $MAPbI_3$ in DMF (496 mg mL^{-1}) and 0.25 M LP surfactant in DMF (0.2 mg mL^{-1})	Blade coating	Glass/ITO/PTAA/PVK/C_{60}/BCP/Cu	57.2	13 × 8.5	14.6[d] (stabilized)	180
276.7 mg PbI_2 in 1 mL DMF or mixed solvent (DMF : additives) (0.6 M) The solution mixture of FAI : MABr : MACl (60 mg : 6 mg : 6 mg in 1 mL IPA) was bladed onto the PbI_2 films	Blade coating	Glass/FTO/SnO_2/PVK/Spiro-OMeTAD/Au	16.54% for 5 × 5 cm^2 perovskite solar modules, and 13.32% for 10 × 10 cm^2 modules			167
The solid $MAPbI_3$ crystals changed to liquid *via* MA gas-assisted solid–liquid transition. The viscous liquid was diluted with ACN in a weight ratio of viscous liquid to ACN = 60 : 40	D-bar coating	Glass/FTO/SnO_2/PVK/Spiro-OMeTAD/Au	10 × 10	10 × 12	Many PCEs[b] were reported (~16-18%)	181
PbI_2 in DMF (0.7 M, 322 mg mL^{-1}) MAI (10 mg mL^{-1}) in IPA	Slot-die coating	PET/ITO/ZnO/PVK/P_3HT/Ag	5 × 8	10 × 10	—	165
40% $MAPbI_3$ in DMF	Slot-die coating	Glass/FTO/ZnO/PVK/home-made carbon paste	17.6	5 × 5	10.6[b]	182

Table 3 (*Contd.*)

Ink recipe (PVK)	Method	Device structure	Active area (cm^2)	Module area (cm^2)	η (%)	Ref.
1 mM of lead compounds $PbCl_2$ and $Pb(CH_3COO)\cdot 3H_2O$ at a molar ratio of 1 : 4 and 3 mM of MAI per 1 mL of DMF	Slot-die coating	Glass/ITO/c-TiO_2/PVK/Spiro-OMeTAD/Au	151.88	12.5 × 13.5	11.1[b]	183
573.0 mg PbI_2, 197.5 mg MAI, and 13.70 mg 5-AVAI in 1.0 mL GBL	Slot-die coating	Glass/FTO/m-TiO_2/ZrO_2/carbon/PVK	60.08	80.55 (aperture area)	12.87[b]	106
0.8 M $MAPbI_{3-x}Cl_x$ in DMF/GBL mixed solvent	Spray coating	Glass/FTO/TiO_2/PVK/PTAA/Au	40	10 × 10	15.5[b]	184
0.15 M $Cs_{0.17}FA_{0.83}PbI_3$ in DMF : DMSO (1 : 2, v/v)	Spray coating	Glass/ITO/NiO/PVK/C_{60}/BCP/Au	5.9	—	15.5[b]	185
0.53 g of PbI_2, 0.19 g of MAI and 0.0176 g of 5-AVAI in 1 mL of GBL	Ink-jet printing	Glass/FTO/TiO_2/ZrO_2/carbon/printed PVK	—	10 × 10 (18 cells)	—	107
1.2 M PbI_2, 1.2 M MAI and 0.06 M 5-AVAI in 1 mL of GBL	Ink-jet printing	Glass/FTO/TiO_2/ZrO_2/carbon/printed PVK	0.64	1.5	9.1[b]	108
L-α-Phosphatidylcholine and methylammonium hypophosphite were added into ≈1.45 M $MAPbI_3$/2-ME solution at a concentration of ≈0.3 mg mL^{-1} and ≈0.15 vol%, respectively	Blade coating	Willow glass/ITO/PTAA/PVK/C_{60}/BCP/Cu	Geometric fill factor 92%	42.9 (aperture area)	15.86[d]	186
1.26 mM PbI_2, 1.26 mM FAI, 0.06 mM $MAPbBr_3$ and 0.5 mM MACl in DMF/DMSO (8 : 1 v/v) mixed solvent	Spin coating	PEN/ITO/np-SnO_2 and porous-ZSO (Zn_2SnO_4)/PVK/Spiro-OMeTAD/Au	PCE of 15.5%, 12.9% and 11.8% on an aperture area[d] of 100 cm^2, 225 cm^2 and 400 cm^2, respectively			187
1.3 M organic cation (0.85 FAI and 0.15 MABr) and 1.4 M mixture of metal lead salts (0.85 PbI_2 and 0.15 $PbBr_2$) in a solvent mixture of DMF/DMSO (4 : 1, v/v)	Spin coating	PET/ITO/SnO_2/PVK/Spiro-OMeTAD/Au	16.07	30	15.22[b]	188
460 mg mL^{-1} PbI_2 in DMF 40 mg mL^{-1} MAI in 2-propanal	Spin coating	Cu foil/CuI/PVK/ZnO/Ag	0.8	—	—	189

[a] PVK = perovskite. [b] PCE based on active area. [c] Not mentioned. [d] PCE based on aperture area.

designs can be potentially achieved on both rigid and flexible-based substrates according to the targeted applications. Table 3 provides a summary of the recently reported scalable device configurations of perovskite solar modules designed using scalable perovskite precursor ink formulations on rigid glass and flexible substrates.

5. Forthcoming directions in precursor inks, technological research, and development of next-generation PSC technology

The progressive research and development of PSCs over the past decade provide future directions and guidelines to overcome the remaining key challenges necessary for reaching commercial breakthroughs imagined for this efficient PV technology as envisioned in Fig. 5.

Among them, the toxicity and environmental impact of traditional lead-based precursor inks pose a challenge for the safe deployment of PSCs. In this regard, not only should the safety protocols but also the effective recycling procedures be chosen for the safe removal of hazardous and toxic materials such as PbI_2 with high yield from the installed panels of PSC technology after their end of life. Interestingly, notable progress has been reported in many scientific reports where effective recycling of PbI_2, methylammonium iodide (MAI) and expensive contact layers has been successfully demonstrated for the lab-sized PSCs.[190–192] These proof-of-concept based striking demonstrations provide pathways in designing effective

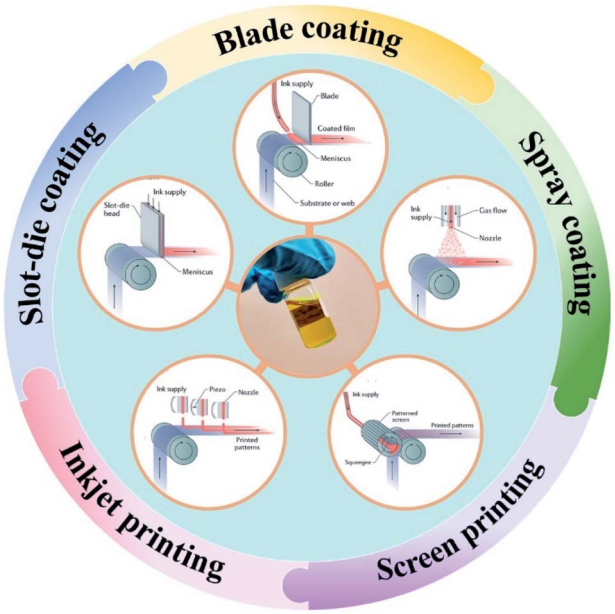

Fig. 4 Some of the popular fabrication schemes opted to produce large area perovskite solar cells and modules. Reproduced from ref. 158 with permission.

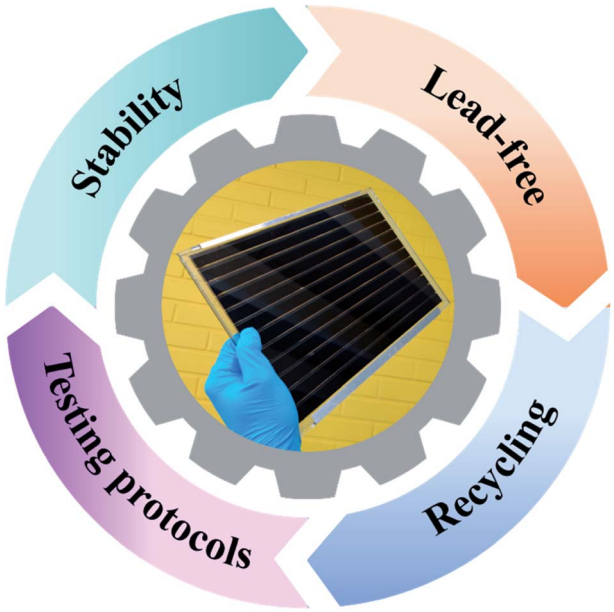

Fig. 5 Summary of the key futuristic directives envisioned for the emerging perovskite solar cell technology.

recycling protocols for large area perovskite solar modules, which may significantly suppress the environmental concerns, which have been heavily debated during the emergence of this low-cost PV technology.[193–195] Moreover, the abundance, availability, cost and sustainability of potential lead compound substitutes and their respective precursor inks must be further investigated to justify their bulk-scale usage to produce the so-called large area eco-friendly perovskite-based PV panels.[196]

On the other hand, despite the growing number of reports on achieving stable photovoltaic performance under various environmental conditions while incorporating advanced perovskite precursor inks,[103,104,197] realistic assessments of PSC device stability based on recently suggested stability testing protocols[197] have yet to be established. Thus far, there are several reports of either stable performances or degradation of initial efficiencies in various device designs of PSCs containing novel precursor inks, using the suggested stability testing protocols for PSC technology. This again raises concerns due to the uncertainty in deploying this emerging PV technology in many suitable applications.

In addition, new consensus statements need to be developed to address advanced stability testing protocols from the perspective of precisely controlled indoor ecological conditions and some severely cold outdoor climatic conditions, which have not been specifically covered in the current stability testing protocols.[8] The possible upcoming deployments of PSC technology in batteryless and maintenance-free IoT devices[198–200] inside modern buildings with precisely controlled ecological conditions or stand-alone communication gadgets in severely cold outdoor climatic conditions call for new testing standards. Notably, degradation rates could vary under such environmental conditions, but these are not known or have rarely been reported to date.

Interesting research questions may provide future research and development directives towards the forthcoming generation of PSC devices over the next decade. Considering the progress that has already been made, it is expected that future technological developments would resolve key research problems of achieving eco-friendly and robust PSC technology with certified integration in vast applications.

6. Summary and conclusions

The development of progressive precursor inks reviewed in this work provides evidence for their contributions towards achieving striking milestones such as high-performance or versatile configuration designs and highlights unique integration possibilities of emerging PSC technology. Moreover, the intelligent precursor inks designed with novel materials reported in the recent past have offered pathways for scalability over both rigid glass and flexible polymer foil-based substrates. As a result, activities related to commercializing PSC technology have greatly accelerated as its integration in smart sensors, charging stations and BIPV based applications continues to be demonstrated.[201]

Nevertheless, additional materials screening is needed for the development of the next generation of novel precursor inks of the perovskite light absorbing layer in order to meet the growing demand, especially from the construction industry where there is keen interest in aesthetically appealing solar panels for smart buildings and nature-friendly ecological architecture.[202–209] This demand may potentially be met by creating precise and flexible patterning that allows individual PSCs to be assembled into aesthetic structures based on solar modules for energy generation.

The current methods such as slot-die coating, spraying or blade coating techniques offer limited flexibility, and have mostly been used to produce serially connected pattern-based modules in traditional n–i–p or p–i–n based device configurations.[188,210,211] Notably, alternative schemes such as drop on demand inkjet printing may provide more freedom of design, since advanced precursor inks of both perovskite-based materials and other active materials can be fabricated to create individual PSCs. These PSCs can be designed with aesthetically attractive arbitrary patterns, which may be intelligently connected to create electricity at targeted watt scales.

Surprisingly, except for the few demonstrations of printing individual active layers[212–215] (including the perovskite-based light absorbing layer[107,216]), inkjet printing has been rarely reported in fabricating complete device designs of PSC technology, despite knowing its potential for fabricating large area-based active layers at high speed. In this regard, one of the most critical limitations realized in producing active layers through inkjet printing is when the nozzles choke the cartridges, which severely limits drop volumes (1–10 picolitres). This in turn makes it difficult to print nanoparticle-based solution processable inks with the necessary precision and resolution. Moreover, the delicate cartridges frequently exhibit chemical incompatibility and often react with the fabricated inks that are composed of novel materials and solvents, thus making it difficult to achieve the desired patterns with ease and accurate precision.[217–220]

These key challenges call for the development of advanced precursor inks to be used with high chemical compatibility, not only to achieve precisely patterned perovskite-based light absorbing layers but also for other active layers to produce fully printed PSC technology with pattern flexibility. One of the potential precursor inks to achieve a perovskite light absorbing layer with high precision has been demonstrated utilizing an inkjet printing technique to produce carbon-based printable perovskite solar cells.[107] The precursor ink showed great compatibility during inkjet printing when fabricated with a novel additive (5-ammonium valeric acid iodide; 5-AVAI), which significantly slows the perovskite crystallization formation and allows the fabricated ink to pass through the inkjet nozzles without reacting with them. Thus far, this stable device configuration[103,105] of PSCs has been demonstrated with schemes such as inkjet printing and screen-printing methods. There is immense potential to achieve further module fabrication with customized designs to generate appealing patterns based on individual cells as discussed earlier in this section.[221]

Hence, a transformation from the first generation of serially connected carbon-based printable perovskite solar modules[106,178] to aesthetically appealing solar panels can be anticipated, which could provide guidelines to produce the next generation of traditional n–i–p and p–i–n configuration-based PSCs, especially when considering evolved design principles. This could assuredly enable realistic outcomes such as the rapid deployment of PSCs worldwide and the resulting positive influence on climate change expected to arise from this promising photovoltaic technology.

Author contributions

C. M. T. K contributed with manuscript planning and communication, writing Sections 1, 2 and 4, drafting tables and figures, screening, and furnishing the manuscript text and references. L. A and M. O contributed with writing and drafting Sections 3 and 5. S. G. H. supervised the research work and contributed with funding acquisition, outline drafting and writing sections, reviewing, and editing the overall manuscript.

Conflicts of interest

The authors have no conflicts to declare.

Acknowledgements

This work was financed by the CAPRINT project (Decision # 2430354811). CMTK and SGH are grateful to the Technology Industries of Finland Centennial Foundation and to the Jane and Aatos Erkko Foundation for financing the doctoral research work and awarding the project funding, respectively. Printed Intelligence Infrastructure is also acknowledged for this work.

References

1 S. Ghasemian, A. Faridzad, P. Abbaszadeh, A. Taklif, A. Ghasemi and R. Hafezi, *Int. J. Environ. Sci. Technol.*, 2020, DOI: 10.1007/s13762-020-02738-5.
2 A. S. World Energy Council and P. S. Institute, *World Energy Resources*, World Energy Counc. Co. Ltd, 2016, pp. 1–138.
3 S. Chu, Y. Cui and N. Liu, *Nat. Mater.*, 2016, **16**, 16–22.
4 Ms. Fitria, *J. Chem. Inf. Model.*, 2013, **53**, 1689–1699.
5 D. Gielen, F. Boshell, D. Saygin, M. D. Bazilian, N. Wagner and R. Gorini, *Energy Strategy Reviews*, 2019, **24**, 38–50.
6 J. Khan and M. H. Arsalan, *Renewable Sustainable Energy Rev.*, 2016, **55**, 414–425.
7 T. M. David, P. M. Silva Rocha Rizol, M. A. Guerreiro Machado and G. P. Buccieri, *Heliyon*, 2020, **6**, e04452.
8 M. Kokkonen, P. Talebi, J. Zhou, S. Asgari, S. A. Soomro, F. Elsehrawy, J. Halme, S. Ahmad, A. Hagfeldt and S. G. Hashmi, *J. Mater. Chem. A*, 2021, **9**, 10527–10545.
9 J. Park, H. Yoo, V. Karade, K. S. Gour, E. Choi, M. Kim, X. Hao, S. J. Shin, J. Kim, H. Shim, D. Kim, J. H. Kim, J. Yun and J. Hyeok Kim, *J. Mater. Chem. A*, 2020, **8**, 14538–14544.
10 S. Biswas and H. Kim, *Polymers*, 2020, **12**, 1338.
11 X. Hou, Y. Wang, H. Ka, H. Lee, R. Datt, N. U. Miano, D. Yan, M. Li, F. Zhu, B. Hou, W. C. Tsoi and Z. Li, *J. Mater. Chem. A*, 2020, 21503–21525.
12 N. G. Park and K. Zhu, *Nat. Rev. Mater.*, 2020, **5**, 333–350.
13 A. S. Gertsen, M. F. Castro, R. R. Søndergaard and J. W. Andreasen, *Flexible Printed Electron.*, 2020, **5**, 014004.
14 E. Aydin, T. G. Allen, M. De Bastiani, L. Xu, J. Ávila, M. Salvador, E. Van Kerschaver and S. De Wolf, *Nat. Energy*, 2020, **5**, 851–859.
15 E. Bellini, Solliance, MiaSolé hit 26.5% efficiency on tandem CIGS/perovskite solar cell, accessed on

16.09.2021, https://www.pv-magazine.com/2021/02/15/solliance-miasole-hit-26-5-efficiency-on-tandem-cigs-perovskite-solar-cell/.
16 A. Aslam, U. Mehmood, M. H. Arshad, A. Ishfaq, J. Zaheer, A. Ul, H. Khan and M. Sufyan, *Sol. Energy*, 2020, **207**, 874–892.
17 Best Research-Cell Efficiency Chart, accessed on 16.09.2021, https://www.nrel.gov/pv/assets/pdfs/best-research-cell-efficiencies.20200104.pdf.
18 A. E. Shalan, *Mater. Adv.*, 2020, **1**, 292–309.
19 J. Yeo and Y. Jeong, *Energy Rep.*, 2020, **6**, 2075–2085.
20 I. Hussain, H. P. Tran, J. Jaksik, J. Moore, N. Islam and M. J. Uddin, *Emergent Mater.*, 2018, **1**, 133–154.
21 A. Mei, X. Li, L. Liu, Z. Ku, T. Liu, Y. Rong, M. Xu, M. Hu, J. Chen, Y. Yang, M. Grätzel and H. Han, *Science*, 2014, **345**, 295–298.
22 J. Su, H. Cai, J. Yang, X. Ye, R. Han, J. Ni, J. Li and J. Zhang, *ACS Appl. Mater. Interfaces*, 2020, **12**, 3531–3538.
23 A. Giuri, S. Masi, A. Listorti, G. Gigli, S. Colella, C. Esposito and A. Rizzo, *Nano Energy*, 2018, **54**, 400–408.
24 J. Li, J. Dagar, O. Shargaieva, M. A. Flatken, H. Köbler, M. Fenske, C. Schultz, B. Stegemann, J. Just, D. M. Többens, A. Abate, R. Munir and E. Unger, *Adv. Energy Mater.*, 2021, **11**, 2003460.
25 N. Vlachopoulos, A. Hagfeldt, I. Benesperi, M. Freitag, G. Hashmi, G. Jia, R. A. Wahyuono, J. Plentz and B. Dietzek, *Sustainable Energy Fuels*, 2021, **5**, 367–383.
26 I. Benesperi, H. Michaels and M. Freitag, *J. Mater. Chem. C*, 2018, **6**, 11903–11942.
27 M. Rai, L. H. Wong and L. Etgar, *J. Phys. Chem. Lett.*, 2020, **11**, 8189–8194.
28 Z. Chen, Q. Dong, Y. Liu, C. Bao, Y. Fang, Y. Lin, S. Tang, Q. Wang, X. Xiao, Y. Bai, Y. Deng and J. Huang, *Nat. Commun.*, 2017, **8**, 1–7.
29 A. Bag, R. Radhakrishnan, R. Nekovei and R. Jeyakumar, *Sol. Energy*, 2020, **196**, 177–182.
30 Y. Hou, W. Chen, D. Baran, T. Stubhan, N. A. Luechinger, B. Hartmeier, M. Richter, J. Min, S. Chen, C. O. R. Quiroz, N. Li, H. Zhang, T. Heumueller, G. J. Matt, A. Osvet, K. Forberich, Z. G. Zhang, Y. Li, B. Winter, P. Schweizer, E. Spiecker and C. J. Brabec, *Adv. Mater.*, 2016, **28**, 5112–5120.
31 J. Chen and N. G. Park, *Adv. Mater.*, 2019, **31**, 1–56.
32 C. M. Wolff, P. Caprioglio, M. Stolterfoht and D. Neher, *Adv. Mater.*, 2019, **31**, 1902762.
33 D. Luo, R. Su, W. Zhang, Q. Gong and R. Zhu, *Nat. Rev. Mater.*, 2020, **5**, 44–60.
34 B. Wang, H. Li, Q. Dai, M. Zhang, Z. Zou, J.-L. Brédas and Z. Lin, *Angew. Chem., Int. Ed.*, 2021, **60**, 17664–17670.
35 T.-S. Su, F. T. Eickemeyer, M. A. Hope, F. Jahanbakhshi, M. Mladenović, J. Li, Z. Zhou, A. Mishra, J.-H. Yum, D. Ren, A. Krishna, O. Ouellette, T.-C. Wei, H. Zhou, H.-H. Huang, M. D. Mensi, K. Sivula, S. M. Zakeeruddin, J. V Milić, A. Hagfeldt, U. Rothlisberger, L. Emsley, H. Zhang and M. Grätzel, *J. Am. Chem. Soc.*, 2020, **142**, 19980–19991.
36 D. Liu, C. J. Traverse, P. Chen, M. Elinski, C. Yang, L. Wang, M. Young and R. R. Lunt, *Adv. Sci.*, 2018, **5**, 1700484.
37 M. Qin, J. Cao, T. Zhang, J. Mai, T. K. Lau, S. Zhou, Y. Zhou, J. Wang, Y. J. Hsu, N. Zhao, J. Xu, X. Zhan and X. Lu, *Adv. Energy Mater.*, 2018, **8**, 1–9.
38 X. Wu, Y. Jiang, C. Chen, J. Guo, X. Kong, Y. Feng, S. Wu, X. Gao, X. Lu, Q. Wang, G. Zhou, Y. Chen, J. M. Liu, K. Kempa and J. Gao, *Adv. Funct. Mater.*, 2020, **30**, 1908613.
39 J. Kim, B. W. Park, J. Baek, J. S. Yun, H. W. Kwon, J. Seidel, H. Min, S. Coelho, S. Lim, S. Huang, K. Gaus, M. A. Green, T. J. Shin, A. W. Y. Ho-Baillie, M. G. Kim and S. Il Seok, *J. Am. Chem. Soc.*, 2020, **142**, 6251–6260.
40 A. Kojima, K. Teshima, Y. Shirai and T. Miyasaka, *J. Am. Chem. Soc.*, 2009, **131**, 6050–6051.
41 G. Wang, D. Liu, J. Xiang, D. Zhou, K. Alameh, B. Ding and Q. Song, *RSC Adv.*, 2016, **6**, 43299–43303.
42 S. M. H. Qaid, M. S. Al Sobaie, M. A. Majeed Khan, I. M. Bedja, F. H. Alharbi, M. K. Nazeeruddin and A. S. Aldwayyan, *Mater. Lett.*, 2016, **164**, 498–501.
43 N. Yantara, F. Yanan, C. Shi, H. A. Dewi, P. P. Boix, S. G. Mhaisalkar and N. Mathews, *Chem. Mater.*, 2015, **27**, 2309–2314.
44 P. Docampo, J. M. Ball, M. Darwich, G. E. Eperon and H. J. Snaith, *Nat. Commun.*, 2013, **4**, 1–6.
45 J. M. Ball, M. M. Lee, A. Hey and H. J. Snaith, *Energy Environ. Sci.*, 2013, **6**, 1739–1743.
46 H. Choi, J. Jeong, H.-B. Kim, S. Kim, B. Walker, G.-H. Kim and J. Y. Kim, *Nano Energy*, 2014, **7**, 80–85.
47 H. S. Kim, C. R. Lee, J. H. Im, K. B. Lee, T. Moehl, A. Marchioro, S. J. Moon, R. Humphry-Baker, J. H. Yum, J. E. Moser, M. Grätzel and N. G. Park, *Sci. Rep.*, 2012, **2**, 1–7.
48 M. M. Lee, J. Teuscher, T. Miyasaka, T. N. Murakami and H. J. Snaith, *Science*, 2012, **338**, 643–647.
49 J. Burschka, N. Pellet, S. J. Moon, R. Humphry-Baker, P. Gao, M. K. Nazeeruddin and M. Grätzel, *Nature*, 2013, **499**, 316–319.
50 N. J. Jeon, J. H. Noh, Y. C. Kim, W. S. Yang, S. Ryu and S. Il Seok, *Nat. Mater.*, 2014, **13**, 897–903.
51 C. G. Wu, C. H. Chiang, Z. L. Tseng, M. K. Nazeeruddin, A. Hagfeldt and M. Grätzel, *Energy Environ. Sci.*, 2015, **8**, 2725–2733.
52 D. Bi, W. Tress, M. I. Dar, P. Gao, J. Luo, C. Renevier, K. Schenk, A. Abate, F. Giordano, J. P. C. Baena, J. D. Decoppet, S. M. Zakeeruddin, M. K. Nazeeruddin, M. Grätzel and A. Hagfeldt, *Sci. Adv.*, 2016, **2**, e1501170.
53 D. Bi, C. Yi, J. Luo, J. D. Décoppet, F. Zhang, S. M. Zakeeruddin, X. Li, A. Hagfeldt and M. Grätzel, *Nat. Energy*, 2016, **1**, 1–5.
54 M. Saliba, T. Matsui, K. Domanski, J.-Y. Seo, A. Ummadisingu, S. M. Zakeeruddin, J.-P. Correa-Baena, W. R. Tress, A. Abate, A. Hagfeldt and M. Grätzel, *Science*, 2016, **354**, 206–209.
55 W. S. Yang, B. W. Park, E. H. Jung, N. J. Jeon, Y. C. Kim, D. U. Lee, S. S. Shin, J. Seo, E. K. Kim, J. H. Noh and S. Il Seok, *Science*, 2017, **356**, 1376–1379.

56 M. Kim, G. H. Kim, T. K. Lee, I. W. Choi, H. W. Choi, Y. Jo, Y. J. Yoon, J. W. Kim, J. Lee, D. Huh, H. Lee, S. K. Kwak, J. Y. Kim and D. S. Kim, *Joule*, 2019, **3**, 2179–2192.
57 M. Jeong, I. W. Choi, E. M. Go, Y. Cho, M. Kim, B. Lee, S. Jeong, Y. Jo, H. W. Choi, J. Lee, J. H. Bae, S. K. Kwak, D. S. Kim and C. Yang, *Science*, 2020, **369**, 1615–1620.
58 J. J. Yoo, G. Seo, M. R. Chua, T. G. Park, Y. Lu, F. Rotermund, Y. K. Kim, C. S. Moon, N. J. Jeon, J. P. Correa-Baena, V. Bulović, S. S. Shin, M. G. Bawendi and J. Seo, *Nature*, 2021, **590**, 587–593.
59 J. Jeong, M. Kim, J. Seo, H. Lu, P. Ahlawat, A. Mishra, Y. Yang, M. A. Hope, F. T. Eickemeyer, M. Kim, Y. J. Yoon, I. W. Choi, B. P. Darwich, S. J. Choi, Y. Jo, J. H. Lee, B. Walker, S. M. Zakeeruddin, L. Emsley, U. Rothlisberger, A. Hagfeldt, D. S. Kim, M. Grätzel and J. Y. Kim, *Nature*, 2021, **592**, 381–385.
60 K. Zhao, Y. Li, H. Cheng, K. Hu and Z. S. Wang, *J. Power Sources*, 2020, **472**, 9–12.
61 S. Yang, H. Zhao, M. Wu, S. Yuan, Y. Han, Z. Liu, K. Guo, S. (Frank) Liu, S. Yang, H. Zhao, S. Yuan, Y. Han, Z. Liu, S. Liu, M. Wu and K. Guo, *Sol. Energy Mater. Sol. Cells*, 2019, **201**, 110052.
62 C. C. Tseng, L. C. Chen, L. B. Chang, G. M. Wu, W. S. Feng, M. J. Jeng, D. W. Chen and K. L. Lee, *Sol. Energy*, 2020, **204**, 270–279.
63 M. I. Saidaminov, K. Williams, M. Wei, A. Johnston, R. Quintero-Bermudez, M. Vafaie, J. M. Pina, A. H. Proppe, Y. Hou, G. Walters, S. O. Kelley, W. A. Tisdale and E. H. Sargent, *Nat. Mater.*, 2020, **19**, 412–418.
64 S. Karthick, H. Hawashin, N. Parou, S. Vedraine, S. Velumani and J. Bouclé, *Sol. Energy*, 2021, **218**, 226–236.
65 N. K. Pendyala, S. Magdassi and L. Etgar, *ACS Appl. Mater. Interfaces*, 2021, **13**, 30524–30532.
66 H. T. Hussein, R. S. Zamel, M. S. Mohamed and M. K. A. Mohammed, *J. Phys. Chem. Solids*, 2021, **149**, 109792.
67 B. Yu, L. Zhang, J. Wu, K. Liu, H. Wu, J. Shi, Y. Luo, D. Li, Z. Bo and Q. Meng, *J. Mater. Chem. A*, 2020, **8**, 1417–1424.
68 X. Li, S. Ke, X. X. Feng, X. Zhao, W. Zhang and J. Fang, *J. Mater. Chem. A*, 2021, **9**, 12684–12689.
69 L. Xu, X. Feng, W. Jia, W. Lv, A. Mei, Y. Zhou, Q. Zhang, R. Chen and W. Huang, *Energy Environ. Sci.*, 2021, **14**, 4292–4317.
70 T. Ye, K. Wang, Y. Hou, D. Yang, N. Smith, B. Magill, J. Yoon, R. R. H. H. Mudiyanselage, G. A. Khodaparast, K. Wang and S. Priya, *J. Am. Chem. Soc.*, 2021, **143**, 4319–4328.
71 K. D. Jayan and V. Sebastian, *Adv. Theory Simul.*, 2021, **4**, 1–11.
72 Z. Xiao and Y. Yan, *Adv. Energy Mater.*, 2017, **7**, 1–20.
73 H. Li, Q. Wei and Z. Ning, *Appl. Phys. Lett.*, 2020, **117**, 060502.
74 J. K. Nam, M. S. Jung, S. U. Chai, Y. J. Choi, D. Kim and J. H. Park, *J. Phys. Chem. Lett.*, 2017, **8**, 2936–2940.
75 A. Bonadio, C. A. Escanhoela, F. P. Sabino, G. Sombrio, V. G. De Paula, F. F. Ferreira, A. Janotti, G. M. Dalpian and J. A. Souza, *J. Mater. Chem. A*, 2021, **9**, 1089–1099.
76 T. Chen, B. J. Foley, C. Park, C. M. Brown, L. W. Harriger, J. Lee, J. Ruff, M. Yoon, J. J. Choi and S. H. Lee, *Sci. Adv.*, 2016, **2**, 1–7.
77 G. Murugadoss, P. Arunachalam, S. K. Panda, M. Rajesh Kumar, J. R. Rajabathar, H. Al-Lohedan and M. D. Wasmiah, *J. Mater. Res. Technol.*, 2021, **12**, 1924–1930.
78 L. Guo, G. Xu, G. Tang, D. Fang and J. Hong, *Nanotechnology*, 2020, **31**, 225204.
79 G. Tong, D. Y. Son, L. K. Ono, H. B. Kang, S. He, L. Qiu, H. Zhang, Y. Liu, J. Hieulle and Y. Qi, *Nano Energy*, 2021, **87**, 106152.
80 D. Huang, P. Xie, Z. Pan, H. Rao and X. Zhong, *J. Mater. Chem. A*, 2019, **7**, 22420–22428.
81 S. Wang, Z. Ma, B. Liu, W. Wu, Y. Zhu, R. Ma and C. Wang, *Sol. RRL*, 2018, **2**, 1–10.
82 N. Ahn, D. Y. Son, I. H. Jang, S. M. Kang, M. Choi and N. G. Park, *J. Am. Chem. Soc.*, 2015, **137**, 8696–8699.
83 Y. Liu, I. Shin, I. W. Hwang, S. Kim, J. Lee, M. S. Yang, Y. K. Jung, J. W. Jang, J. H. Jeong, S. H. Park and K. H. Kim, *ACS Appl. Mater. Interfaces*, 2017, **9**, 12382–12390.
84 L. A. Frolova, A. I. Davlethanov, N. N. Dremova, I. Zhidkov, A. F. Akbulatov, E. Z. Kurmaev, S. M. Aldoshin, K. J. Stevenson and P. A. Troshin, *J. Phys. Chem. Lett.*, 2020, **11**, 6772–6778.
85 J. W. Lee, D. J. Seol, A. N. Cho and N. G. Park, *Adv. Mater.*, 2014, **26**, 4991–4998.
86 M. B. Johansson, L. Xie, B. J. Kim, J. Thyr, T. Kandra, E. M. J. Johansson, M. Göthelid, T. Edvinsson and G. Boschloo, *Nano Energy*, 2020, **78**, 105346.
87 B. A. Al-Asbahi, S. M. H. Qaid, M. Hezam, I. Bedja, H. M. Ghaithan and A. S. Aldwayyan, *Opt. Mater.*, 2020, **103**, 109836.
88 T. Niu, J. Lu, M. C. Tang, D. Barrit, D. M. Smilgies, Z. Yang, J. Li, Y. Fan, T. Luo, I. McCulloch, A. Amassian, S. Liu and K. Zhao, *Energy Environ. Sci.*, 2018, **11**, 3358–3366.
89 H.-C. Liao, P. Guo, C.-P. Hsu, M. Lin, B. Wang, L. Zeng, W. Huang, C. M. M. Soe, W.-F. Su, M. J. Bedzyk, M. R. Wasielewski, A. Facchetti, R. P. H. Chang, M. G. Kanatzidis and T. J. Marks, *Adv. Energy Mater.*, 2017, **7**, 1601660.
90 L. Tzounis, T. Stergiopoulos, A. Zachariadis, C. Gravalidis, A. Laskarakis and S. Logothetidis, *Mater. Today: Proc.*, 2017, **4**, 5082–5089.
91 X. Dong, D. Chen, J. Zhou, Y. Z. Zheng and X. Tao, *Nanoscale*, 2018, **10**, 7218–7227.
92 H. Kim, H. R. Byun and M. S. Jeong, *Sci. Rep.*, 2019, **9**, 1–7.
93 H. X. Dang, K. Wang, M. Ghasemi, M. C. Tang, M. De Bastiani, E. Aydin, E. Dauzon, D. Barrit, J. Peng, D. M. Smilgies, S. De Wolf and A. Amassian, *Joule*, 2019, **3**, 1746–1764.
94 S. Moghadamzadeh, I. M. Hossain, T. Duong, S. Gharibzadeh, T. Abzieher, H. Pham, H. Hu, P. Fassl,

U. Lemmer, B. A. Nejand and U. W. Paetzold, *J. Mater. Chem. A*, 2020, **8**, 24608–24619.
95 Y. Yu, C. Wang, C. R. Grice, N. Shrestha, D. Zhao, W. Liao, L. Guan, R. A. Awni, W. Meng, A. J. Cimaroli, K. Zhu, R. J. Ellingson and Y. Yan, *ACS Energy Lett.*, 2017, **2**, 1177–1182.
96 S. Ham, Y. J. Choi, J. W. Lee, N. G. Park and D. Kim, *J. Phys. Chem. C*, 2017, **121**, 3143–3148.
97 G. Tang, P. You, Q. Tai, R. Wu and F. Yan, *Sol. RRL*, 2018, **2**, 1–9.
98 J. Chen, S. G. Kim, X. Ren, H. S. Jung and N. G. Park, *J. Mater. Chem. A*, 2019, **7**, 4977–4987.
99 M. J. Choi, Y. S. Lee, I. H. Cho, S. S. Kim, D. H. Kim, S. N. Kwon and S. I. Na, *Nano Energy*, 2020, **71**, 104639.
100 A. Mishra and Z. Ahmad, *J. Mater. Sci.: Mater. Electron.*, 2019, **30**, 20320–20329.
101 D. Zheng, C. Tong, T. Zhu, Y. Rong and T. Pauporté, *Nanomaterials*, 2020, **10**, 1–15.
102 S. M. P. Meroni, C. Worsley, D. Raptis and T. M. Watson, *Energies*, 2021, 14.
103 G. Grancini, C. Roldán-Carmona, I. Zimmermann, E. Mosconi, X. Lee, D. Martineau, S. Narbey, F. Oswald, F. De Angelis, M. Graetzel and M. K. Nazeeruddin, *Nat. Commun.*, 2017, **8**, 1–8.
104 Y. Sheng, W. Ji, Y. Chu, Y. Ming, A. Mei, Y. Hu, Y. Rong and H. Han, *Sol. RRL*, 2020, **4**, 1–7.
105 A. Mei, Y. Sheng, Y. Ming, Y. Hu, Y. Rong, W. Zhang, S. Luo, G. Na, C. Tian, X. Hou, Y. Xiong, Z. Zhang, S. Liu, S. Uchida, T.-W. Kim, Y. Yuan, L. Zhang, Y. Zhou and H. Han, *Joule*, 2020, **4**, 2646–2660.
106 M. Xu, W. Ji, Y. Sheng, Y. Wu, H. Cheng, J. Meng, Z. Yan, J. Xu, A. Mei, Y. Hu, Y. Rong and H. Han, *Nano Energy*, 2020, **74**, 1–8.
107 S. G. Hashmi, D. Martineau, X. Li, M. Ozkan, A. Tiihonen, M. I. Dar, T. Sarikka, S. M. Zakeeruddin, J. Paltakari, P. D. Lund and M. Grätzel, *Adv. Mater. Technol.*, 2017, **2**, 4–9.
108 A. Verma, D. Martineau, S. Abdolhosseinzadeh, J. Heier and F. Nüesch, *Mater. Adv.*, 2020, **1**, 153–160.
109 S. Bai, P. Da, C. Li, Z. Wang, Z. Yuan, F. Fu, M. Kawecki, X. Liu, N. Sakai, J. T. W. Wang, S. Huettner, S. Buecheler, M. Fahlman, F. Gao and H. J. Snaith, *Nature*, 2019, **571**, 245–250.
110 L. Zhou, Z. Lin, Z. Ning, T. Li, X. Guo, J. Ma, J. Su, C. Zhang, J. Zhang, S. Liu, J. Chang and Y. Hao, *Sol. RRL*, 2019, **3**, 1–10.
111 C. Gao, H. Dong, X. Bao, Y. Zhang, A. Saparbaev, L. Yu, S. Wen, R. Yang and L. Dong, *J. Mater. Chem. C*, 2018, **6**, 8234–8241.
112 F. Liu, X. Zuo, K. Wang, H. Bao, L. Liu, Z. Guo, S. Wang and S. F. Liu, *Sol. RRL*, 2021, **5**, 1–10.
113 L. Chao, T. Niu, H. Gu, Y. Yang, Q. Wei, Y. Xia, W. Hui, S. Zuo, Z. Zhu, C. Pei, X. Li, J. Zhang, J. Fang, G. Xing, H. Li, X. Huang, X. Gao, C. Ran, L. Song, L. Fu, Y. Chen and W. Huang, *Research*, 2020, **2020**, 2616345.
114 T. Niu, L. Chao, W. Gao, C. Ran, L. Song, Y. Chen, L. Fu and W. Huang, *ACS Energy Lett.*, 2021, **6**, 1453–1479.
115 L. Chao, Y. Xia, B. Li, G. Xing, Y. Chen and W. Huang, *Chem*, 2019, **5**, 995–1006.
116 N. Park, *Nature Sustainability*, 2021, **4**, 192–193.
117 T. Bu, L. Wu, X. Liu, X. Yang, P. Zhou, X. Yu, T. Qin, J. Shi, S. Wang, S. Li, Z. Ku, Y. Peng, F. Huang, Q. Meng, Y.-B. Cheng and J. Zhong, *Adv. Energy Mater.*, 2017, **7**, 1700576.
118 Q. Zhang, F. Hao, J. Li, Y. Zhou, Y. Wei and H. Lin, *Sci. Technol. Adv. Mater.*, 2018, **19**, 425–442.
119 R. Guo, B. Dahal, A. Thapa, Y. R. Poudel, Y. Liu and W. Li, *Nanoscale Adv.*, 2021, **3**, 2056–2064.
120 H. Zhu, Y. Ren, L. Pan, O. Ouellette, F. T. Eickemeyer, Y. Wu, X. Li, S. Wang, H. Liu, X. Dong, S. M. Zakeeruddin, Y. Liu, A. Hagfeldt and M. Grätzel, *J. Am. Chem. Soc.*, 2021, **143**, 3231–3237.
121 J. Li, H.-L. Cao, W.-B. Jiao, Q. Wang, M. Wei, I. Cantone, J. Lü and A. Abate, *Nat. Commun.*, 2020, **11**, 310.
122 M. Krebs-Moberg, M. Pitz, T. L. Dorsette and S. H. Gheewala, *Renewable Energy*, 2021, **164**, 556–565.
123 T. Ibn-Mohammed, S. C. L. Koh, I. M. Reaney, A. Acquaye, G. Schileo, K. B. Mustapha and R. Greenough, *Renewable Sustainable Energy Rev.*, 2017, **80**, 1321–1344.
124 R. Vidal, J. Alberola-Borràs, N. Sánchez-Pantoja and I. Mora-Seró, *Advanced Energy and Sustainability Research*, 2021, **2**, 2000088.
125 L. Gollino and T. Pauporté, *Sol. RRL*, 2021, **5**, 1–28.
126 M. Wang, W. Wang, B. Ma, W. Shen, L. Liu, K. Cao, S. Chen and W. Huang, *Lead-Free Perovskite Materials for Solar Cells*, Springer, Singapore, 2021, vol. 13.
127 K. Nishimura, M. A. Kamarudin, D. Hirotani, K. Hamada, Q. Shen, S. Iikubo, T. Minemoto, K. Yoshino and S. Hayase, *Nano Energy*, 2020, **74**, 104858.
128 T. Wu, X. Liu, X. He, Y. Wang, X. Meng, T. Noda, X. Yang and L. Han, *Sci. China: Chem.*, 2020, **63**, 107–115.
129 Z. Jin, B. Bin Yu, M. Liao, D. Liu, J. Xiu, Z. Zhang, E. Lifshitz, J. Tang, H. Song and Z. He, *J. Energy Chem.*, 2021, **54**, 414–421.
130 I. Kopacic, B. Friesenbichler, S. F. Hoefler, B. Kunert, H. Plank, T. Rath and G. Trimmel, *ACS Appl. Energy Mater.*, 2018, **1**, 343–347.
131 N. Ito, M. A. Kamarudin, D. Hirotani, Y. Zhang, Q. Shen, Y. Ogomi, S. Iikubo, T. Minemoto, K. Yoshino and S. Hayase, *J. Phys. Chem. Lett.*, 2018, **9**, 1682–1688.
132 A. Singh, P. T. Lai, A. Mohapatra, C. Y. Chen, H. W. Lin, Y. J. Lu and C. W. Chu, *Chem. Eng. J.*, 2021, **419**, 129424.
133 N. Giesbrecht, A. Weis and T. Bein, *J. Phys Energy*, 2020, **2**, 024007.
134 Y. Yang, C. Liu, M. Cai, Y. Liao, Y. Ding, S. Ma, X. Liu, M. Guli, S. Dai and M. K. Nazeeruddin, *ACS Appl. Mater. Interfaces*, 2020, **12**, 17062–17069.
135 W. Hu, X. He, Z. Fang, W. Lian, Y. Shang, X. Li, W. Zhou, M. Zhang, T. Chen, Y. Lu, L. Zhang, L. Ding and S. Yang, *Nano Energy*, 2020, **68**, 104362.
136 D. B. Khadka, Y. Shirai, M. Yanagida and K. Miyano, *J. Mater. Chem. C*, 2019, **7**, 8335–8343.
137 F. Bai, Y. Hu, Y. Hu, T. Qiu, X. Miao and S. Zhang, *Sol. Energy Mater. Sol. Cells*, 2018, **184**, 15–21.

138 J. Li, J. Duan, X. Yang, Y. Duan, P. Yang and Q. Tang, *Nano Energy*, 2021, **80**, 105526.
139 X. Liu, T. Wu, J. Y. Chen, X. Meng, X. He, T. Noda, H. Chen, X. Yang, H. Segawa, Y. Wang and L. Han, *Energy Environ. Sci.*, 2020, **13**, 2896–2902.
140 Z. Yang, M. Zhong, Y. Liang, L. Yang, X. Liu, Q. Li, J. Zhang and D. Xu, *Adv. Funct. Mater.*, 2019, **29**, 1903621.
141 W. Ke, P. Priyanka, S. Vegiraju, C. C. Stoumpos, I. Spanopoulos, C. M. M. Soe, T. J. Marks, M. C. Chen and M. G. Kanatzidis, *J. Am. Chem. Soc.*, 2018, **140**, 388–393.
142 Z. Chen, B. Turedi, A. Y. Alsalloum, C. Yang, X. Zheng, I. Gereige, A. Alsaggaf, O. F. Mohammed and O. M. Bakr, *ACS Energy Lett.*, 2019, **4**, 1258–1259.
143 Y. Zhang, S. Seo, S. Y. Lim, Y. Kim, S. G. Kim, D. K. Lee, S. H. Lee, H. Shin, H. Cheong and N. G. Park, *ACS Energy Lett.*, 2020, 360–366.
144 Y. Wang, X. Liu, T. Zhang, X. Wang, M. Kan, J. Shi and Y. Zhao, *Angew. Chem., Int. Ed.*, 2019, **58**, 16691–16696.
145 M. Saliba, T. Matsui, J. Y. Seo, K. Domanski, J. P. Correa-Baena, M. K. Nazeeruddin, S. M. Zakeeruddin, W. Tress, A. Abate, A. Hagfeldt and M. Grätzel, *Energy Environ. Sci.*, 2016, **9**, 1989–1997.
146 E. H. Jung, N. J. Jeon, E. Y. Park, C. S. Moon, T. J. Shin, T. Y. Yang, J. H. Noh and J. Seo, *Nature*, 2019, **567**, 511–515.
147 J. J. Yoo, S. Wieghold, M. C. Sponseller, M. R. Chua, S. N. Bertram, N. T. P. Hartono, J. S. Tresback, E. C. Hansen, J. P. Correa-Baena, V. Bulović, T. Buonassisi, S. S. Shin and M. G. Bawendi, *Energy Environ. Sci.*, 2019, **12**, 2192–2199.
148 E. Jung, K. Budzinauskas, S. Öz, F. Ünlü, H. Kuhn, J. Wagner, D. Grabowski, B. Klingebiel, M. Cherasse, J. Dong, P. Aversa, P. Vivo, T. Kirchartz, T. Miyasaka, P. H. M. Van Loosdrecht, L. Perfetti and S. Mathur, *ACS Energy Lett.*, 2020, **5**, 785–792.
149 F. Zhang, D. Bi, N. Pellet, C. Xiao, Z. Li, J. J. Berry, S. M. Zakeeruddin, K. Zhu and M. Grätzel, *Energy Environ. Sci.*, 2018, **11**, 3480–3490.
150 N. Li, S. Tao, Y. Chen, X. Niu, C. K. Onwudinanti, C. Hu, Z. Qiu, Z. Xu, G. Zheng, L. Wang, Y. Zhang, L. Li, H. Liu, Y. Lun, J. Hong, X. Wang, Y. Liu, H. Xie, Y. Gao, Y. Bai, S. Yang, G. Brocks, Q. Chen and H. Zhou, *Nat. Energy*, 2019, **4**, 408–415.
151 C. H. Ng, K. Nishimura, N. Ito, K. Hamada, D. Hirotani, Z. Wang, F. Yang, S. likubo, Q. Shen, K. Yoshino, T. Minemoto and S. Hayase, *Nano Energy*, 2019, **58**, 130–137.
152 N. Pai, J. Lu, T. R. Gengenbach, A. Seeber, A. S. R. Chesman, L. Jiang, D. C. Senevirathna, P. C. Andrews, U. Bach, Y. B. Cheng and A. N. Simonov, *Adv. Energy Mater.*, 2019, **9**, 1–11.
153 F. D. Giacomo, H. Fledderus, H. Gorter, G. Kirchner, I. d. Vries, I. Dogan, W. Verhees, V. Zardetto, M. Najafi, D. Zhang, H. Lifka, Y. Galagan, T. Aernouts, S. Veenstra, P. Groen and R. Andriesse, in *2018 IEEE 7th World Conference on Photovoltaic Energy Conversion (WCPEC) (A Joint Conference of 45th IEEE PVSC, 28th PVSEC & 34th EU PVSEC)*, 2018, pp. 2795–2798.
154 X. Li, D. Bi, C. Yi, J.-D. Décoppet, J. Luo, S. M. Zakeeruddin, A. Hagfeldt and M. Grätzel, *Science*, 2016, **353**, 58–62.
155 Q. He, K. Yao, X. Wang, X. Xia, S. Leng and F. Li, *ACS Appl. Mater. Interfaces*, 2017, **9**, 41887–41897.
156 C. Li, J. Yin, R. Chen, X. Lv, X. Feng, Y. Wu and J. Cao, *J. Am. Chem. Soc.*, 2019, **141**, 6345–6351.
157 G. Li, Y. Jiang, S. Deng, A. Tam, P. Xu, M. Wong and H.-S. Kwok, *Adv. Sci.*, 2017, **4**, 1700463.
158 Z. Li, T. R. Klein, D. H. Kim, M. Yang, J. J. Berry, M. F. A. M. van Hest and K. Zhu, *Nat. Rev. Mater.*, 2018, **3**, 18017.
159 P. Zhao, B. J. Kim, X. Ren, D. G. Lee, G. J. Bang, J. B. Jeon, W. Bin Kim and H. S. Jung, *Adv. Mater.*, 2018, **30**, 1802763.
160 W. Qiu, T. Merckx, M. Jaysankar, C. Masse de la Huerta, L. Rakocevic, W. Zhang, U. W. Paetzold, R. Gehlhaar, L. Froyen, J. Poortmans, D. Cheyns, H. J. Snaith and P. Heremans, *Energy Environ. Sci.*, 2016, **9**, 484–489.
161 T. Bu, X. Liu, R. Chen, Z. Liu, K. Li, W. Li, Y. Peng, Z. Ku, F. Huang, Y.-B. Cheng and J. Zhong, *J. Mater. Chem. A*, 2018, **6**, 6319–6326.
162 F. Matteocci, S. Razza, F. Di Giacomo, S. Casaluci, G. Mincuzzi, T. M. Brown, A. D'Epifanio, S. Licoccia and A. Di Carlo, *Phys. Chem. Chem. Phys.*, 2014, **16**, 3918–3923.
163 J. Seo, S. Park, Y. Chan Kim, N. J. Jeon, J. H. Noh, S. C. Yoon and S. Il Seok, *Energy Environ. Sci.*, 2014, **7**, 2642–2646.
164 S. Razza, F. D. Giacomo, F. Matteocci, L. Cinà, A. L. Palma, S. Casaluci, P. Cameron, A. D'Epifanio, S. Licoccia, A. Reale, T. M. Brown and A. D. Carlo, *J. Power Sources*, 2015, **277**, 286–291.
165 K. Hwang, Y.-S. Jung, Y.-J. Heo, F. H. Scholes, S. E. Watkins, J. Subbiah, D. J. Jones, D.-Y. Kim and D. Vak, *Adv. Mater.*, 2015, **27**, 1241–1247.
166 G. Cotella, J. Baker, D. Worsley, F. De Rossi, C. Pleydell-Pearce, M. Carnie and T. Watson, *Sol. Energy Mater. Sol. Cells*, 2017, **159**, 362–369.
167 J. Zhang, T. Bu, J. Li, H. Li, Y. Mo, Z. Wu, Y. Liu, X.-L. Zhang, Y.-B. Cheng and F. Huang, *J. Mater. Chem. A*, 2020, **8**, 8447–8454.
168 Y. Deng, X. Zheng, Y. Bai, Q. Wang, J. Zhao and J. Huang, *Nat. Energy*, 2018, **3**, 560–566.
169 F. Di Giacomo, S. Shanmugam, H. Fledderus, B. J. Bruijnaers, W. J. H. Verhees, M. S. Dorenkamper, S. C. Veenstra, W. Qiu, R. Gehlhaar, T. Merckx, T. Aernouts, R. Andriessen and Y. Galagan, *Sol. Energy Mater. Sol. Cells*, 2018, **181**, 53–59.
170 Y. Hu, S. Si, A. Mei, Y. Rong, H. Liu, X. Li and H. Han, *Sol. RRL*, 2017, **1**, 1600019.
171 NEDO and Toshiba develops world's largest film-based perovskite photovoltaic module – 703 cm^2 module achieves 11.7% power conversion efficiency, accessed on 16.09.2021, https://www.global.toshiba/ww/technology/corporate/rdc/rd/topics/18/1806-03.html.
172 G. Overton, Saule prints flexible perovskite solar modules with consistent 10% efficiency, accessed on 16.09.2021, https://www.laserfocusworld.com/detectors-imaging/article/14035450/saule-prints-flexible-perovskite-solar-modules-with-consistent-10-efficiency.

173 T. Bu, S. Shi, J. Li, Y. Liu, J. Shi, L. Chen, X. Liu, J. Qiu, Z. Ku, Y. Peng, J. Zhong, Y.-B. Cheng and F. Huang, *ACS Appl. Mater. Interfaces*, 2018, **10**, 14922–14929.
174 S. Hong, G. Kim, B. Park, J.-H. Kim, J. Kim, Y. Pak, J. Kim, S. Kwon and K. Lee, *J. Mater. Chem. A*, 2020, **8**, 18659–18667.
175 A. Agresti, S. Pescetelli, A. L. Palma, A. E. Del Rio Castillo, D. Konios, G. Kakavelakis, S. Razza, L. Cinà, E. Kymakis, F. Bonaccorso and A. Di Carlo, *ACS Energy Lett.*, 2017, **2**, 279–287.
176 A. Priyadarshi, L. J. Haur, P. Murray, D. Fu, S. Kulkarni, G. Xing, T. C. Sum, N. Mathews and S. G. Mhaisalkar, *Energy Environ. Sci.*, 2016, **9**, 3687–3692.
177 G. Grancini, C. Roldán-Carmona, I. Zimmermann, E. Mosconi, X. Lee, D. Martineau, S. Narbey, F. Oswald, F. De Angelis, M. Graetzel and M. K. Nazeeruddin, *Nat. Commun.*, 2017, **8**, 15684.
178 F. De Rossi, J. A. Baker, D. Beynon, K. E. A. Hooper, S. M. P. Meroni, D. Williams, Z. Wei, A. Yasin, C. Charbonneau, E. H. Jewell and T. M. Watson, *Adv. Mater. Technol.*, 2018, **3**, 1800156.
179 M. Yang, Z. Li, M. O. Reese, O. G. Reid, D. H. Kim, S. Siol, T. R. Klein, Y. Yan, J. J. Berry, M. F. A. M. van Hest and K. Zhu, *Nat. Energy*, 2017, **2**, 17038.
180 Y. Deng, X. Zheng, Y. Bai, Q. Wang, J. Zhao and J. Huang, *Nat. Energy*, 2018, **3**, 560–566.
181 D. N. Jeong, D. K. Lee, S. Seo, S. Y. Lim, Y. Zhang, H. Shin, H. Cheong and N. G. Park, *ACS Energy Lett.*, 2019, **4**, 1189–1195.
182 L. Cai, L. Liang, J. Wu, B. Ding, L. Gao and B. Fan, *J. Semicond.*, 2017, **38**, 014006.
183 F. Di, S. Shanmugam, H. Fledderus, B. J. Bruijnaers, W. J. H. Verhees, M. S. Dorenkamper, S. C. Veenstra and W. Qiu, *Sol. Energy Mater. Sol. Cells*, 2018, **181**, 53–59.
184 J. H. Heo, M. H. Lee, M. H. Jang and S. H. Im, *J. Mater. Chem. A*, 2016, **4**, 17636–17642.
185 N. Rolston, W. J. Scheideler, A. C. Flick, J. P. Chen, H. Elmaraghi, A. Sleugh, O. Zhao, M. Woodhouse and R. H. Dauskardt, *Joule*, 2020, **4**, 2675–2692.
186 X. Dai, Y. Deng, C. H. Van Brackle, S. Chen, P. N. Rudd, X. Xiao, Y. Lin, B. Chen and J. Huang, *Adv. Energy Mater.*, 2020, **10**, 1903108.
187 J. Chung, S. S. Shin, K. Hwang, G. Kim, K. W. Kim, D. S. Lee, W. Kim, B. S. Ma, Y.-K. Kim, T.-S. Kim and J. Seo, *Energy Environ. Sci.*, 2020, **13**, 4854–4861.
188 T. Bu, J. Li, F. Zheng, W. Chen, X. Wen, Z. Ku, Y. Peng, J. Zhong, Y.-B. Cheng and F. Huang, *Nat. Commun.*, 2018, **9**, 4609.
189 B. Abdollahi Nejand, P. Nazari, S. Gharibzadeh, V. Ahmadi and A. Moshaii, *Chem. Commun.*, 2017, **53**, 747–750.
190 F. Yang, S. Wang, P. Dai, L. Chen, A. Wakamiya and K. Matsuda, *J. Mater. Chem. A*, 2021, **9**, 2612–2627.
191 F.-W. Liu, G. Biesold, M. Zhang, R. Lawless, J.-P. Correa-Baena, Y.-L. Chueh and Z. Lin, *Mater. Today*, 2021, **43**, 185–197.
192 B. J. Kim, D. H. Kim, S. L. Kwon, S. Y. Park, Z. Li, K. Zhu and H. S. Jung, *Nat. Commun.*, 2016, **7**, 11735.
193 S.-Y. Bae, S. Y. Lee, J. Kim, H. N. Umh, J. Jeong, S. Bae, J. Yi, Y. Kim and J. Choi, *Sci. Rep.*, 2019, **9**, 4242.
194 A. Urbina, *J. Phys. Energy*, 2020, **2**, 22001.
195 R. Vidal, J.-A. Alberola-Borràs, N. Sánchez-Pantoja and I. Mora-Seró, *Advanced Energy and Sustainability Research*, 2021, **2**, 2000088.
196 G. Schileo and G. Grancini, *J. Mater. Chem. C*, 2021, **9**, 67–76.
197 M. V. Khenkin, E. A. Katz, A. Abate, G. Bardizza, J. J. Berry, C. Brabec, F. Brunetti, V. Bulović, Q. Burlingame, A. Di Carlo, R. Cheacharoen, Y. B. Cheng, A. Colsmann, S. Cros, K. Domanski, M. Dusza, C. J. Fell, S. R. Forrest, Y. Galagan, D. Di Girolamo, M. Grätzel, A. Hagfeldt, E. von Hauff, H. Hoppe, J. Kettle, H. Köbler, M. S. Leite, S. (Frank) Liu, Y. L. Loo, J. M. Luther, C. Q. Ma, M. Madsen, M. Manceau, M. Matheron, M. McGehee, R. Meitzner, M. K. Nazeeruddin, A. F. Nogueira, Ç. Odabaşı, A. Osherov, N. G. Park, M. O. Reese, F. De Rossi, M. Saliba, U. S. Schubert, H. J. Snaith, S. D. Stranks, W. Tress, P. A. Troshin, V. Turkovic, S. Veenstra, I. Visoly-Fisher, A. Walsh, T. Watson, H. Xie, R. Yıldırım, S. M. Zakeeruddin, K. Zhu and M. Lira-Cantu, *Nat. Energy*, 2020, **5**, 35–49.
198 S. Castro-Hermosa, G. Lucarelli, M. Top, M. Fahland, J. Fahlteich and T. M. Brown, *Cell Rep. Phys. Sci.*, 2020, **1**, 100045.
199 X. He, J. Chen, X. Ren, L. Zhang, Y. Liu, J. Feng, J. Fang, K. Zhao and S. Liu, *Adv. Mater.*, 2021, **2100770**, 1–10.
200 Versatility of Solar PV Technology: Saule Technologies to Provide Perovskite Solar Cells for Animal Tracking Devices under WWF Project to Save European Bison, accessed on 16.09.2021, http://taiyangnews.info/technology/wwf-project-to-use-solar-cell-powered-animal-trackers/.
201 Products-Saule Technologies, accessed on 16.09.2021, https://sauletech.com/product/.
202 Y. Zhu, L. Shu, Q. Zhang, Y. Zhu, S. Poddar, C. Wang, Z. He and Z. Fan, *EcoMat*, 2021, **3**, e12117, DOI: 10.1002/eom2.12117, accessed on 16.09.2021.
203 S. Kim, J. Yi and J. Kim, *Sol. RRL*, 2021, **5**, 2100162.
204 H. Alaa and N. Gharib, *IOP Conf. Ser.: Mater. Sci. Eng.*, 2020, **974**, 12020, DOI: 10.1088/1757-899X/974/1/012020.
205 A. Y. Foo, M. H. Saw, Y. S. Khoo and S. E. R. Tay, in *2021 IEEE 48th Photovoltaic Specialists Conference (PVSC)*, 2021, pp. 272–277, accessed on 16.09.2021, https://ieeexplore.ieee.org/document/9518916.
206 D. Hardy, in *PLEA 2013 Sustainable Architecture for a Renewable Future*, 2013, accessed on 16.09.2021, https://www.researchgate.net/publication/284639897_Improving_the_Aesthetics_of_Photovoltaics_Through_Use_of_Coloured_Encapsulants.
207 S. Conejos, M. Y. L. Chew, K. Tay, S. Tay and S. Safiena, *Int. J. Build. Pathol. Adapt.*, DOI: 10.1108/IJBPA-04-2019-0038.
208 S. A. Al-Janahi, S. G. Al-Ghamdi, Environmental Impact Associated with the Performance of Building Integrated Photovoltaics: Life-Cycle Assessment Perspective, in *Energy Systems EvaluationEnergy and Technology*, 2021, ed.

J. Ren, Green Energy and Technology, Springer, Cham, vol. 1.

209 P. Corti, P. Bonomo, F. Frontini, P. Mace, E. Bosch, *Building Integrated Photovoltaics: A practical handbook for solar buildings' stakeholders*, 2020.

210 L.-H. Chou, Y.-T. Yu, I. Osaka, X.-F. Wang and C.-L. Liu, *J. Power Sources*, 2021, **491**, 229586.

211 S. Razza, F. Di Giacomo, F. Matteocci, L. Cinà, A. L. Palma, S. Casaluci, P. Cameron, A. D'Epifanio, S. Licoccia, A. Reale, T. M. Brown and A. Di Carlo, *J. Power Sources*, 2015, **277**, 286–291.

212 F. Schackmar, H. Eggers, M. Frericks, B. S. Richards, U. Lemmer, G. Hernandez-Sosa and U. W. Paetzold, *Adv. Mater. Technol.*, 2021, **6**, 2000271.

213 A. Verma, D. Martineau, S. Abdolhosseinzadeh, J. Heier and F. Nüesch, *Mater. Adv.*, 2020, **1**, 153–160.

214 N. K. Pendyala, S. Magdassi and L. Etgar, *ACS Appl. Mater. Interfaces*, 2021, **13**, 30524–30532.

215 F. Mathies, H. Eggers, B. S. Richards, G. Hernandez-Sosa, U. Lemmer and U. W. Paetzold, *ACS Appl. Energy Mater.*, 2018, **1**, 1834–1839.

216 L. Zhang, S. Chen, X. Wang, D. Wang, Y. Li, Q. Ai, X. Sun, J. Chen, Y. Li, X. Jiang, S. Yang and B. Xu, *Sol. RRL*, 2021, **5**, 2100106.

217 J. R. Castrejón-Pita, W. R. S. Baxter, J. Morgan, S. Temple, G. D. Martin and I. M. Hutchings, *Atomization Sprays*, 2013, **23**, 571–595.

218 A. A. Castrejón-Pita, J. R. Castrejón-Pita and G. D. Martin, *Rev. Sci. Instrum.*, 2012, **83**, 115105.

219 T. Lamminmäki, J. Kettle, H. Rautkoski, A. Kokko and P. Gane, *Ind. Eng. Chem. Res.*, 2011, **50**, 7251–7263.

220 M. Makrygianni, A. Milionis, C. Kryou, I. Trantakis, D. Poulikakos and I. Zergioti, *Adv. Mater. Interfaces*, 2018, **5**, 1800440.

221 H. Sebastian, Master thesis, Aalto University, 2021, accessed on 16.09.2021, https://aaltodoc.aalto.fi/handle/123456789/107031.